

A MATHEMATICAL MODEL FOR PREDICTION  
OF DOWNHOLE GAS WELL UNIFORM  
CORROSION IN CO<sub>2</sub> AND H<sub>2</sub>S  
CONTAINING BRINES

By

GUOHAI LIU

Bachelor of Science  
East China Institute of Chemical  
Technology  
Shanghai, China  
1982

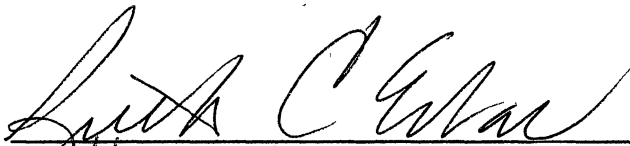
Master of Science  
Central Coal Mining Research Institute  
Beijing, China  
1984

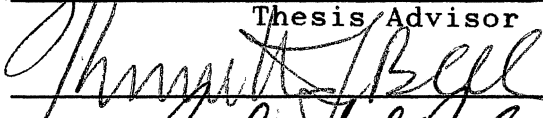
Submitted to the Faculty of the  
Graduate College of the  
Oklahoma State University  
in partial fulfillment of  
the requirements for  
the Degree of  
DOCTOR OF PHILOSOPHY  
December, 1991

Thesis  
1991D  
L783m


A MATHEMATICAL MODEL FOR PREDICTION  
OF DOWNHOLE GAS WELL UNIFORM  
CORROSION IN CO<sub>2</sub> AND H<sub>2</sub>S  
CONTAINING BRINES

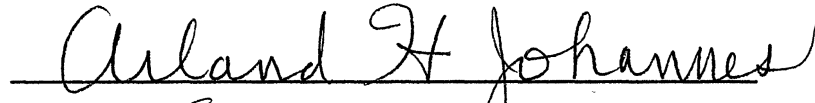
Thesis Approved:

  
\_\_\_\_\_  
Thesis Advisor

  
\_\_\_\_\_

  
\_\_\_\_\_

  
\_\_\_\_\_

  
\_\_\_\_\_

  
\_\_\_\_\_  
Dean of the Graduate College

## ACKNOWLEDGMENTS

I wish to express my sincere gratitude to all the people who helped me in the course of my study at Oklahoma State University. I am deeply indebted to my thesis advisor, Dr. Ruth. C. Erbar, for her intelligent guidance, encouragement, patience, and invaluable help and support through the three years of this work. Without her help, this work would not have been possible.

I am also thankful to Drs. Kenneth J. Bell, Frank W. Chambers, Arland H. Johannes and Robert L. Robinson Jr. for serving as my committee members and for their advisement. Having the opportunity to associate with these mentors will have a permanent influence on my whole academic career.

A special note of appreciation is due for the financial support from the industrial sponsors, Amoco, Arco, Conoco, Marathon, Norsk Hydro, ORYX and Phillips, through the School of Chemical Engineering.

My wife, Jinjuan and my son, Su, deserve my deepest appreciation for their encouragement and understanding in spite of never knowing when the end of my busy days would be.

Finally, my parents deserve my admiration for their confidence in their son through thick or thin.

## TABLE OF CONTENTS

Chapter	Page
I. INTRODUCTION . . . . .	1
II. LITERATURE SURVEY . . . . .	5
Downhole Corrosion Phenomena . . . . .	5
Mechanisms of Downhole Corrosion . . . . .	9
Electrochemical Reaction Mechanisms of H <sub>2</sub> S and CO <sub>2</sub> Corrosion . . . . .	9
Mechanisms of Mass Transfer in the Corrosion Processes . . . . .	23
Modeling Downhole Corrosion. . . . .	27
Summary of the Literature Survey . . . . .	29
III. MODEL DESCRIPTION . . . . .	30
Physical Model . . . . .	30
Model Formulations . . . . .	35
The Interface of the Gas and Liquid . . . . .	35
Mass Transfer Through Turbulent Film Layer . . . . .	42
Mass Transfer and Ion Migration Through Diffusion Layer . . . . .	51
Mass Transfer Through the Corrosion Product Layer . . . . .	53
Kinetics of Surface Reactions . . . . .	53
IV. NUMERICAL SOLUTIONS OF THE SYSTEM MODEL . . . . .	59
Solution of Gas and Liquid Interface . . . . .	59
Solution of Mass Transfer Through Turbulent Layer. . . . .	60
Solution of Diffusion Layer Model. . . . .	61
Overall Computational Strategy . . . . .	64
V. RESULTS AND DISCUSSIONS . . . . .	66
The Effect of CO <sub>2</sub> and H <sub>2</sub> S Partial Pressure . . . . .	66
The Effect of Flow Rate. . . . .	77
Some Downhole Cases. . . . .	81
Case I . . . . .	81
Case II . . . . .	87
Case III. . . . .	92

Chapter	Page
Case IV . . . . .	99
Case V. . . . .	.102
VI. CONCLUSIONS AND RECOMMENDATIONS . . . . .	.112
Conclusions. . . . .	.112
Recommendations. . . . .	.114
Modeling Localized Corrosion. . . . .	.114
Modeling of the Gas Wells with Condensate. . . . .	.115
Prediction of the Effect of the Inhibitor . . . . .	.115
Experimental Research on the Corrosion Rate Under Slug Flow. . . . .	.116
REFERENCES . . . . .	.117

## LIST OF TABLES

Table	Page
I. Temperature Coefficients for Equilibrium Constants . . . . .	38
II. Temperature Coefficients for Henry's Constants. . . . .	39
III. Values of $b_i$ for Some Species in Equation (3.21). . . . .	40
IV. Gas Composition of the Well for Case I. . . . .	82
V. Water Analysis of Gas Well for Case I . . . . .	83
VI. Well Conditions for Case I. . . . .	84
VII. Gas Composition of the Well for Case II . . . . .	88
VIII. Water Analysis of Gas Well for Case II. . . . .	89
IX. Well Conditions for Case II . . . . .	90
X. Gas Composition of the Well for Case III. . . . .	93
XI. Water Analysis of Gas Well for Case III . . . . .	94
XII. Well Conditions for Case III. . . . .	95
XIII. Gas Composition of the Well for Case IV . . . . .	100
XIV. Well Conditions for Case IV . . . . .	101
XV. Assumed Gas Composition for Case V. . . . .	104
XVI. Water Analysis of Gas Well for Case V . . . . .	105
XVII. Well Conditions for Case V. . . . .	106

## LIST OF FIGURES

Figure	Page
1. Schematic Diagram of Downhole Annular Two-Phase Gas-Liquid Flow . . . . .	31
2. Composite Structure of Corrosion Processes for Annular Two Phase Flow. . . . .	34
3. Flow Chart of Downhole Corrosion Program. . . . .	65
4. The Influence of CO <sub>2</sub> Partial Pressure on Corrosion Rate at 60 C Without Film . . . . .	67
5. The Influence of CO <sub>2</sub> Partial Pressure on Corrosion Rate at 90 C Without Film . . . . .	68
6. The Influence of H <sub>2</sub> S Partial Pressure on Corrosion Rate at 25 C Without Film . . . . .	71
7. The Influence of CO <sub>2</sub> Partial Pressure on Corrosion Rate at 25 C with Film. . . . .	73
8. The Influence of H <sub>2</sub> S Partial Pressure on Corrosion Rate at 25 C with Film. . . . .	76
9. The Influence of Liquid Flow Rate on Corrosion Rate at 60 C in 4% NaCl Without Film. . . . .	78
10. The Influence of Liquid Flow Rate on Corrosion Rate at 60 C in 4% NaCl with Film . . . . .	80
11. The Corrosion Rate Profile Along Depth for Case I. . . . .	85
12. The Corrosion Rate Profile Along Depth for Case II . . . . .	91
13. The Corrosion Rate Profile Along Depth for Case III. . . . .	96
14. The Corrosion Rate Profile Along Depth for Case III with Protective Film. . . . .	97



Figure	Page
15. The Corrosion Rate Profile Along Depth for Case I with Protective Film . . . . .	98
16. The Corrosion Rate Profile Along Depth for Case IV with Protective Film . . . . .	.103
17. The Corrosion Rate Profile Along Depth for Case V Without Protective Film . . . . .	.108
18. The Corrosion Rate Profile Along Depth for Case V with Protective Film . . . . .	.110

## NOMENCLATURE

A	coefficient in equation (3.46)
$A_j$	temperature coefficients of equilibrium constants
$A_s$	coefficient in equation (2.1)
$A_\phi$	Debye-Huckel parameter
B	constant in equation (2.1)
$b_a$	anodic Tafel constant
$b_i$	coefficient in equation (3.21)
$b_k$	cathodic Tafel constant
$C_i$	activity of i component
$C_{i,s}$	activity of i component at the wall
$C_{i,1}$	activity of i component at the interface of turbulent layer and diffusion layer
D	diameter of the pipe
$D_i$	diffusion coefficients of i species
$D^+$	dimensionless diameter $Du^*/v_L$
$E_{corr}$	corrosion potential
$E_{e,m}$	equilibrium potential of anodic reaction
$E_{e,so}$	equilibrium potential of cathodic reactions
F	Faraday's constant
$F_o$	dimensionless group defined by equation (3.53)
f	average friction factor in the liquid film

$f_i$	fugacity coefficients of gas phase
$f_{t1}$	interfacial friction factor
$g$	gravitational acceleration
$H$	Henry's constant
$h$	step size
$I$	ionic strength
$I_i$	corrosion current density
$I_m$	mixing length
$I_m^+$	dimensionless mixing length
$i_a$	anodic current density
$i_{a0}$	anodic exchange current density
$i_c$	corrosion current in (2.1)
$i_{c1}, i_{c2}$	cathodic current densities
$i_{c10}, i_{c20}$	cathodic exchange current densities
$K_{1,CO_2}$	the first dissociation constant of $H_2CO_3$
$K_{2,CO_2}$	the second dissociation constant of $H_2CO_3$
$K_{1,H_2S}$	the first dissociation constant of $H_2S$
$K_{2,H_2S}$	the second dissociation constant of $H_2S$
$K_L$	mass transfer coefficient in liquid film
$K^+$	dimensionless mass transfer coefficient, $K_L/u^*$
$k_s$	wall roughness
$k_s^+$	dimensionless wall roughness, $k_s u^*/\nu_L$
$K_{sp,CaCO_3}$	activity product of $CaCO_3$
$K_{sp,FeCO_3}$	activity product of $FeCO_3$
$K_{sp,FeS}$	activity product of $FeCO_3$
$K_w$	the dissociation constant of $H_2O$

$m_i$	molality of $i$ component
$N_1$	dimensionless group defined by equation (3.56)
$N_i$	mass flux of $i$ component
$P$	total pressure
$R$	radius of the pipe
$R$	universal gas constant
$Re_c$	core fluid Reynolds number $4(W_g + W_{LE}) / \pi(d-2\delta)\mu_c$
$Re_f$	liquid film Reynolds number, $4W_{LF} / \pi\mu_L D$
$Re_g$	gas phase superficial Reynolds number
$r_i$	core radius
$Sc$	Schmidt number
$Sh$	Sherwood Number, $K_L \delta / D_i$
$t$	temperature in degree C
$T$	absolute temperature K
$U$	liquid film velocity
$U_{av}$	average liquid film velocity
$U_c$	gas core velocity
$U^+$	dimensionless liquid film velocity, $U/u^*$
$u_i$	mobility of $i$ species
$u^*$	wall friction velocity $(\tau_w / \rho_L)^{1/2}$
$V$	total volume of vapor phase
$W_g$	mass flow rate of gas phase
$W_{LE}$	mass flow rate of droplets
$W_{LF}$	mass flow rate of liquid film
$x$	droplet mass fraction in the gas phase

$y$	wall coordinate
$y_{CO_2}$	mole fraction of $CO_2$ in gas phase
$y_{H_2O}$	mole fraction of $H_2O$ in gas phase
$y_{H_2S}$	mole fraction of $H_2S$ in gas phase
$y_i$	mole fraction of $i$ component in gas phase
$y^*$	dimensionless wall coordinate
$Z_i$	charge number of $i$ species
$z$	axial coordinate
$\alpha_a$	anodic reaction transfer coefficient
$\alpha_{c1}, \alpha_{c2}$	cathodic reaction transfer coefficients
$\beta$	function of $Re_f$ defined by equation (3.54)
$\delta$	average liquid film thickness
$\delta_1$	diffusion layer thickness
$\delta^*$	dimensionless liquid film thickness, $\delta u^*/\nu_L$
$\epsilon_D$	eddy diffusivity for mass transfer
$\eta$	dimensionless liquid film thickness, $y/\delta$
$\eta'$	dimensionless wall coordinate shift in equation (3.38)
$\eta_a$	anodic overpotential
$\eta_c$	cathodic overpotential
$\mu_L$	liquid viscosity
$\mu_c$	core fluid viscosity, $x\mu_L + (1-x)\mu_g$
$\mu_t$	turbulent viscosity
$\nu_L$	liquid kinematic viscosity
$\nu_t$	turbulent kinematic viscosity
$\rho_c$	core fluid density

$\rho_L$	liquid density
$\rho_g$	gas density
$\tau$	shear stress
$\tau_i$	interfacial shear stress
$\tau_w$	wall shear stress
$\Phi$	electric potential

## CHAPTER I

### INTRODUCTION

Many oil and/or gas fields produce varying amounts of carbon dioxide ( $\text{CO}_2$ ), hydrogen sulfide ( $\text{H}_2\text{S}$ ) and water. These gases dissolved into water form a weak acid that is found to be corrosive. The corrosive medium may cause severe downhole corrosion of various types. Fontana (1986) has classified corrosion into eight forms. Most of the eight forms of corrosion may occur downhole. Broadly speaking, downhole corrosion can be categorized into uniform and localized corrosion. Uniform or general corrosion causes overall metal loss and general thinning of metal due to chemical and/or mechanical actions. Localized corrosion has the appearance of pits or grooves.

The complication of downhole corrosion lies in the complex fluid flow and phase behavior of the well fluids. Generally speaking, a gas and/or oil well can produce three fluids (oil, water and gas). Corrosion only occurs when water phase is contact with metal. Even for those gas wells producing negligible condensate, the two-phase flow (water and gas) phenomena are not very clear in terms of the effect on corrosion. For example, almost all the experimental data on corrosion are taken from single phase

flow. How can these data be applied to downhole two phase flow?

Having CO<sub>2</sub>, H<sub>2</sub>S and water produced downhole, the corrosion in gas and oil production operations depends on many factors, such as CO<sub>2</sub> and H<sub>2</sub>S concentration in the gas phase, system pressure and temperature, the presence of solid contamination, the properties of corrosion product film, the phase behavior and fluid velocity, two-phase flow regime, concentrations of various inorganic ions in the formation water, etc.. The influence of these parameters and interactions among them is a very important aspect in the corrosion research on oil and gas production systems.

The severity of downhole corrosion and its economic impact on oil and gas production have motivated the broad range of experimental research and field observations worldwide in the past four decades or so. National Association of Corrosion Engineers (NACE) has compiled most of the related research data up to 1985 in four books (Tuttle and Kane, 1981, Newton and Hausler, 1984, Hausler and Godard 1984, and Burke et al., 1985). A review of this literature reveals that the areas covered are mainly on the basic mechanisms, field experience in combating the corrosion problems, and empirical correlations of corrosion rate.

The prediction of downhole corrosion includes physically describing the system and the mathematical



formulation of this description. Both aspects present formidable tasks. The difficulty in setting up the physical model lies in that to the observer the downhole system is a "black box". Therefore, all the descriptions of the phenomena are, at best, "intelligently" speculative. In fact, up to this date many phenomena occurring downhole have not been understood properly. The second difficulty is obvious since handling multiphase turbulent flow, mass transfer, and multicomponent heterogeneous reactions simultaneously is mathematically a hard nut to crack. Therefore, the prediction of downhole corrosion must be from an oversimplified model with further simplified mathematical treatments.

Notwithstanding the difficulty in the prediction of downhole corrosion, the need for such prediction is still attractive for the research. As has been pointed out by Crolet and Bonis (1984), the prediction of corrosion includes not only predicting the risk of corrosion but also predicting the possibility of a lack of corrosion since, for a new well, one has to decide what materials should be used for the pipe downhole. Reliable predictions can probably reduce operating costs and completion costs. For example, using stainless steel for a noncorrosive well is a very costly luxury.

The purpose of this thesis is to develop a mathematical model that can be used to predict downhole

uniform corrosion of gas wells in CO<sub>2</sub> and H<sub>2</sub>S containing brines. Here, uniform corrosion is studied because not only it is relatively simple but also it forms a basis for the further investigation of localized corrosion. Within a certain theoretical framework and the associated assumptions, this model will include most parameters that have influence on the corrosion rate mentioned previously.

The model results were compared with some experimental data. These will provide some insight into further theoretical and experimental research on downhole corrosion.

## CHAPTER II

### LITERATURE SURVEY

The problem of downhole corrosion in CO<sub>2</sub> and H<sub>2</sub>S containing brines covers a wide area and has been investigated for several decades. A survey of the literature shows that multiple parameters affect the downhole corrosion rate. Much progress has been made in basic research but many problems need to be cleared up. In terms of the prediction of the downhole corrosion rate few publications have appeared in the literature. In the following a brief description of some related work will be given.

#### Downhole Corrosion Phenomena

The corrosion of steel equipment in oil and gas production systems has been found to be a problem since the 1940s. Bacon and Brown (1943) reported serious cases of corrosion in some gas wells. They found that the corrosion occurred immediately downstream from the various fittings and orifice plates in the internal pipe surface. The gas produced contained about 1% CO<sub>2</sub> and traces of H<sub>2</sub>S. The pH of the produced water was from 5.0 to 6.0 at the wellhead. From this information, one can reason that the damage to

the pipe is probably due to the erosion-corrosion by the highly turbulent two-phase swirling flow downstream of the fittings.

Hackermann and Shock (1947) studied the properties of the surface corrosion product layers formed on coupons exposed in the well head. They found that, qualitatively speaking, there are three types of surface layers on the coupons. For noncorrosive wells the surface layer is thin, adherent, and apparently nonporous. For corrosive wells, one type of film is made of thick, adherent, porous layers which are conducive to pit formation and cause serious problems of local corrosion. Another type of film is of thicker, porous layers which are, however, nonadherent. These findings clearly showed that the corrosion product films depend on the characteristics of the corrosive medium. This conclusion was also confirmed in laboratory experiments by Shoesmith et al. (1980) who studied the initial stages of corrosion of iron by unstirred saturated H<sub>2</sub>S solutions at 21 °C as a function of pH.

Since the 1950s, extensive field observations have been made for downhole corrosion in aqueous CO<sub>2</sub> and H<sub>2</sub>S solutions. A survey of the literature ( Braburn 1977, Burke and Hausler 1985, Crolet 1983, Crolet and Bonis 1984, Gatzke and Hausler 1984, Hausler and Burke 1985, Houghton and Westermarck 1983, Hudson 1989, Martin 1988, Rice 1989, Rogers et al. 1990, Shock and Sudbury 1951, Smith 1982,

Speel 1976, Thompson et al. 1991, Tuttle 1987, 1990, Weeter 1964, Zitter 1973) reveals that there are many factors affecting the rate of corrosion in oil and gas wells. The types of corrosion are also varied, including uniform corrosion, pitting corrosion, erosion-corrosion, hydrogen embrittlement, and stress corrosion cracking etc., depending upon the corrosive environment. The observed phenomena in downhole corrosion from the literature cited above can be summarized as follows:

1. The corrodent gases, H<sub>2</sub>S and CO<sub>2</sub>, dissolve in the water phase and acidify the water phase. The acidified water accelerates tubing corrosion.
2. Under two-phase flow, erosion-corrosion can occur at lower average fluid velocity than with single phase flow.
3. The severe localized corrosion may appear at various corrosive conditions.
4. The gas and water production rate have an important influence on the corrosion rate.
5. The inorganic ions in the brines have some influence on the corrosion rate.

This general summary is quite obvious. However, the causes of these phenomena have not been explained satisfactorily in the literature cited above.

Some authors (Shock and Sudbury 1951, Smith 1982, Zitter 1973, Tuttle 1987, 1990) believe that the partial

pressures of H<sub>2</sub>S and CO<sub>2</sub> are the most important index in the prediction of corrosiveness of a well. This index is based on the observation that at lower pH (pH < 4) the corrosion rate is very high and the dissolution of H<sub>2</sub>S and CO<sub>2</sub> results in lowering the pH of the brine. According to this index, generally, the system is considered to be corrosive if the partial pressure of corrosive gases is above 15 psi. It may also be corrosive if the partial pressure is between 7-15 psi. Below 7 psi partial pressure the system is considered noncorrosive. It can be expected that in a system as complex as that for downhole corrosion there would be a lot of exceptions to this simple index. Therefore, Bradurn (1977) proposed water production rate as an index to determine the corrosion rate and found that this index correlated with the downhole corrosion rate better than did CO<sub>2</sub> partial pressure. This index has been extended (Gatzke and Hausler 1984, Hausler and Burke 1985, and Burke and Hausler 1985) to include the gas production rate. These later authors concluded that H<sub>2</sub>S and CO<sub>2</sub> partial pressures and the total solids in the brines are only minor factors compared with the production rate. Furthermore, Cronet (1983) and Cronet and Bonis (1984) emphasized that, besides temperature, partial pressures of CO<sub>2</sub> and H<sub>2</sub>S, and fluid velocity, the physical chemistry of production water is certainly an important parameter that should be taken into account. In fact, that the downhole

two-phase flow pattern probably is another factor should be considered. Johnson et al. (1991) have observed that slug flow enhances the corrosion rate by a factor of seven compared to annular flow.

These field observations and the economic impact of corrosion of oil and gas wells have provided some inspiration to study the mechanisms of CO<sub>2</sub> and H<sub>2</sub>S corrosion. It is also necessary to understand the corrosion mechanisms to develop any quantitative corrosion model. Therefore, some research results for corrosion mechanisms will be discussed.

### Mechanisms of Downhole Corrosion

#### Electrochemical Reaction Mechanisms of H<sub>2</sub>S and CO<sub>2</sub> Corrosion

The electrochemical reactions occurring on the tube walls have been studied for a long time to try to achieve some understanding of the phenomena. The main concern here is mechanisms of uniform corrosion. Therefore, only those research efforts related to this aspect will be discussed.

De Waard and Milliams (1975) studied the corrosion rate of X-52 carbon steel at different CO<sub>2</sub> partial pressures (up to 1 atm.) and temperatures (up to 80 °C). Based on the experimental evidence that a carbonic acid solution can be more corrosive than the usual mineral acid at the same pH, De Waard and Milliams explored the possible

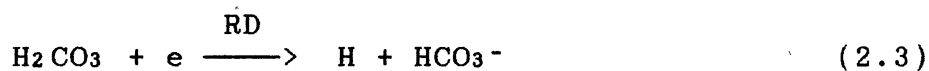
reaction mechanisms. They reasoned that the relation between corrosion current ( $i_c$ ) and pH can always be shown to be of the form

$$\log i_c = - A_s \text{pH} + B \quad (2.1)$$

with

$$A_s = \frac{2b_k - b_a}{b_k + b_a} \quad (2.2)$$

when the hydrogen ion is involved in corrosion reactions. Through measuring both the anodic Tafel constant  $b_a$  ( $b_a = 40$  mv) and the cathodic constant ( $b_k = 120$  mv) they obtained the experimental value of  $A_s$  to be 1.3. On the basis of this fact the authors deduced the following cathodic reaction mechanism:

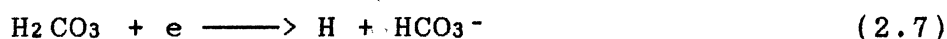


with reaction (2.3) as rate determining step. For this mechanism a value of 1.25 is obtained theoretically for  $A_s$ , which does not differ significantly from the experimental



value of 1.3. One can easily see that the consistency of the value of constant  $A_s$  between the experimental and the theoretical value is no guarantee that the mechanism is correct. It is merely one of the possible mechanisms.

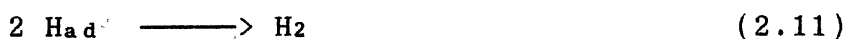
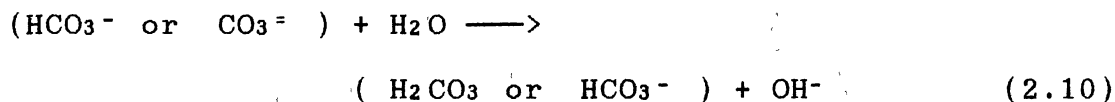
Schmitt and Rothmann (1977), based on their experimental evidence, suggested that the following reactions may occur simultaneously



The experimental support for this mechanism is that hydrogen permeation in  $\text{CO}_2$  corrosion is important. In fact, this mechanism is almost the same as the one proposed by De Waard and Milliams (1975) since the hydrogen evolution reaction is also included in the latter model but is not the rate determining step.

Wieckowski et al. (1983a) reexamined the mechanisms for the reduction of dissolved carbon dioxide proposed previously. The investigations used cyclic voltammetry measurements on static and rotating disk iron electrodes. They proposed that both  $\text{H}_2\text{CO}_3$  and  $\text{HCO}_3^-$  reductions occur on the metal surface through the following mechanism:





This mechanism is an adoption of the general EC' reaction (electron transfer reactions, here 2.8 and 2.9, preceded a homogeneous chemical reaction, here 2.10, with a nonelectroactive species as catalyst, here H<sub>2</sub>O) (Bard and Faulkner 1980). In the framework of this mechanism, both undissociated carbonic acid molecules and HCO<sub>3</sub><sup>-</sup> are regenerated through "catalytic" reactions. The strong argument for this mechanism is that the cathodic current under unstirred conditions is higher than the current recorded in the stirred solutions. This is consistent with the general behavior of the EC' mechanism. However, the higher uniform corrosion rate in the static solution than in the flowing or stirred system is reported nowhere else in the literature. Therefore, the argument is not confirmed by other authors.

The mechanism proposed by Wieckowski et al. (1983a) does not contradict the mechanisms proposed by De Waard and

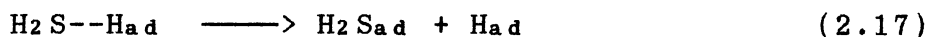
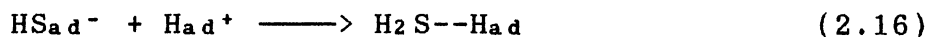
Milliams (1975) and Schmitt and Rothmann (1977), since it was noticed that the reduction of  $\text{HCO}_3^-$  occurs only when there is a corrosion product on the surface (Wieckowski et al. 1983b). The presence of the corrosion product layer, which separates the adsorbed  $\text{H}_2\text{CO}_3$  molecules from the active metal surface, will create a very high field strength ( $10^6$ - $10^7$  V/cm) within the film (Vetter 1967). This high field probably facilitates the transport of  $\text{HCO}_3^-$  and its reduction on the active surface. This point will be returned to later.

The mechanisms of corrosion of steel by  $\text{H}_2\text{S}$  aqueous solutions are almost the same as that of  $\text{CO}_2$  systems. Morris et al. (1980) have investigated steel corrosion through polarization studies in aqueous  $\text{H}_2\text{S}$  systems using a rotating disk electrode cell. The basic experimental evidence showed that, in the presence of  $\text{H}_2\text{S}$ , the Tafel slopes of the anodic and cathodic processes within the pH range examined does not change but the corrosion potential of steel becomes more negative. They proposed that the following reactions may proceed simultaneously



It may be noticed that this mechanism is almost the same as that in CO<sub>2</sub> systems (equations 2.6 and 2.7) proposed by Schmitt and Rothmann (1977).

Kawashima et al. (1976) proposed the following mechanism for corrosion of mild steel by aqueous H<sub>2</sub>S

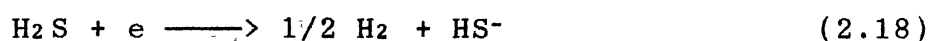


Although this mechanism is based on the experimental data of hydrogen embrittlement, it can be used in the study of uniform corrosion since uniform corrosion precedes hydrogen embrittlement. In fact, the source of hydrogen for the embrittlement of steel is definitely from the corrosion reactions which release hydrogen. This is one of the mechanisms based on the estimated kinetic parameters. In this mechanism, the molecular H<sub>2</sub>S adsorbed on the steel will act as a bridge-forming ligand for the proton discharge. They also showed that H<sub>2</sub>S did not change the Tafel slopes of the anodic and cathodic reactions but did decrease the cathodic overpotential in acid solutions. Comparison of this mechanism with that proposed by

Wieckowski et al. (1983a) for aqueous CO<sub>2</sub> systems (equations 2.8-2.11) shows clear similarity in terms of both H<sub>2</sub>S and HS<sup>-</sup> taking part in the surface reactions.

More recently, Iyer et al. (1990) performed cathodic hydrogen charging experiments in perchloric acid solutions with pH values of 1 and 2 with H<sub>2</sub>S. They confirmed the mechanism proposed by Kawashima et al. (1976). They also observed that H<sub>2</sub>S can slow the hydrogen recombination reaction.

Even further similarity of the mechanisms between the corrosion of steel in CO<sub>2</sub> and H<sub>2</sub>S aqueous solutions can be seen from the work of Bolmer (1965), Shoesmith et al. (1980) and Wikjord et al. (1980). All these authors suggested that the overall reaction is as follows:



This is identical to the mechanism proposed by De Waard and Millianms (1975) for the CO<sub>2</sub> corrosion system (equations 2.3-2.5).

From above discussion, it seems that the presence of H<sub>2</sub>S and CO<sub>2</sub> in solutions does not change the Tafel slopes of either the anodic or cathodic processes. However, H<sub>2</sub>S and CO<sub>2</sub> shift the anodic and cathodic potentials toward the more negative direction. This effect means that both H<sub>2</sub>S and CO<sub>2</sub> accelerate the corrosion rate exponentially. The

reaction mechanisms always involve hydrogen evolution. The reaction path may be  $\text{H}_2\text{S}$  and  $\text{CO}_2$  direct reduction on the metal surfaces. Under certain conditions  $\text{HCO}_3^-$  and/or  $\text{HS}^-$  reductions could occur as corrosion reactions.  $\text{H}^+$  discharge may also occur to some degree in the system.

All the discussions of reaction mechanisms are based on the active wall reactions. In other words, the mechanisms proposed are applicable to the cases where no corrosion product layer was built up on the wall. As mentioned before, Wieckowski et al. (1983) have noticed that the reduction of  $\text{HCO}_3^-$  only occurred when there was a corrosion product on the wall. In fact, in the corrosion processes, reactions occurring on the active wall are only part of the story. The whole picture is that after a certain period of fast reaction on the active wall there would be reaction products build-up on the wall. The corrosion products generally have two roles to play in the corrosion processes. This corrosion product layer can retard the corrosion rate by either acting as a diffusion barrier or by changing the energy status of the metal wall. On the other hand, the corrosion product layer may be porous and leave some part of metal wall in contact with corrosion medium. Under this latter circumstance, the corrosion rate may be worse than that of the whole metal wall with no product film at all owing to the galvanic coupling effect. This is the basic mechanism of pitting

corrosion (Greene and Fontana 1959, Galvele 1983) which will not be discussed here. In the following, the uniform corrosion mechanisms of steel with product films will be discussed.

Ewing (1955) made the first attempt to explain through thermodynamic theory the mechanism of steel corrosion in H<sub>2</sub>S aqueous systems with an iron sulfide corrosion product layer. Although his starting point is quite wrong from the modern point of view and his theory does not explain experimental phenomena well, a few of his speculations are quite to the point. He realized that the changing pH will change the precipitation processes. Further, he estimated that iron sulfide deposition will change the surface potential and that the ratio of ferrous ion to sulfide ion is an important index to assess the properties of the surface and the corrosion rate.

Some of Ewing's (1955) points were confirmed by Meyer et al. (1958), who studied the relations between corrosion rates and different forms of sulfide corrosion products. Meyer et al. (1958) identified three different forms of iron sulfide as corrosion products. They assume that these corrosion products retard corrosion processes by forming diffusion barriers.

Greco and Wright (1962), Sardisco et al. (1963) and Sardisco and Pitts (1965) have made some studies of the mechanism of corrosion of steel in the H<sub>2</sub>S-CO<sub>2</sub>-H<sub>2</sub>O system.

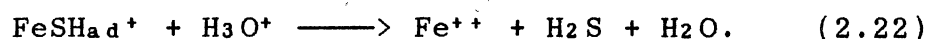
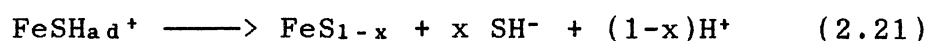
They found in such a system that the corrosion product film consists of FeS<sub>2</sub>, FeS and Fe<sub>9</sub>S<sub>8</sub>, all of which may be formed initially. However, the number of crystallites of each compound formed and/or the rate at which each grew was probably different, depending upon the H<sub>2</sub>S concentration. They also reasoned, based on experimental data, that the overall reaction is made up of contributions from both interface reactions and from diffusion and migration of ions and electrons across the film. At low H<sub>2</sub>S concentration the diffusion part makes the main contribution to the overall reaction and at high H<sub>2</sub>S concentrations the mechanism of the overall reaction tends to be controlled by interface processes. This reasoning is probably wrong. Since higher H<sub>2</sub>S concentrations will render the surface reaction faster, the diffusion effect would be more significant in the overall corrosion rate.

Recently, Shoesmith et al. (1980) and Pound et al. (1989) have made some further studies of the corrosion mechanisms for the steel in H<sub>2</sub>S aqueous solutions. They explored the formation mechanisms of various forms of iron sulfide. Shoesmith et al. (1980) proposed that the anodic reaction occurs by the sequential chemisorption of H<sub>2</sub>S:





The reaction (2.20) may take place in two one-electron steps either forming a growing solid layer of mackinawite ( $\text{FeS}_{1-x}$ , Tetragonal) or hydrolyzing to yield a dissolved species as follows:



Shoesmith et al. (1980) suggested that the anodic reaction with a protective layer is controlled by transport through the base layer of mackinawite at higher current value between pH value 4-5. Mass transfer of  $\text{Fe}^{++}$  and/or  $\text{H}_2\text{S}$  within pores and cracks in this base layer is the most likely polarizing mechanism, since the anodic reaction, at least, will occur on the limited area of exposed metal. Pound et al. (1989) have confirmed the mechanism proposed by Shoesmith et al. through cyclic voltammogram experiments. They further explained the mechanism for forming different types of iron sulfide.

Eriksrud and Sontverdt (1984) have studied various effects on corrosion rates in both formation and synthetic water systems in the presence of  $\text{CO}_2$ . They found that  $\text{FeCO}_3$  is the main constituent in the protective layer. This layer is somewhat more protective with increasing  $\text{Ca}^{++}$

concentration in the solution at constant  $\text{HCO}_3^-$  concentration. The protective layers formed can be removed by the moving gas/liquid mixture in slug flow. They believe that the corrosion mechanism is the same as that proposed by De Waard and Milliams (1975) whether there is a protective film or not. They also reasoned that the corrosion product layer forms a diffusion barrier to ion diffusion and can be influenced by instantaneous wall shear stress exerted by the fluids on the metal surface, thus causing mechanical fatigue action on the protective film.

Some other workers ( Ikeda et al. 1984, 1985, Dunlop et al. 1984, Masamura et al. 1984, Hausler 1984, Xia et al. 1989, Choi et al. 1989, Valand and sjøwall 1989, Palacios and Shadley 1991, Jasinski 1987, Videm and Dugstad 1987) have made extensive studies of the corrosion mechanisms with an  $\text{FeCO}_3$  film on the metal surface. These authors' results are summarized in the following. The film composition formed on the surface is mainly  $\text{FeCO}_3$ . The formation mechanisms are either by direct formation through the following reaction



or through the precipitation reaction



At this stage it is still hard to confirm which reaction dominates. Recent work by Palacios and Shadley (1991) showed that generally there are two layers of corrosion products on the steel surface. A "primary" (inner) layer is formed through reaction (2.23) and a secondary (outer) layer on top of the primary layer is due to recrystallization of iron carbonate reaction (2.24). Some other minor components may exist in the film. Xia et al. (1989) found that both ferrous hydrogen carbonate,  $\text{Fe}(\text{HCO}_3)_2$ , and iron carbonate,  $\text{FeCO}_3$ , were in the corrosion product for short time exposures. More prolonged exposures may reduce  $\text{Fe}(\text{HCO}_3)_2$  to  $\text{FeCO}_3$ . Jasinski (1987) and Videm and Dugstad (1987) have detected iron carbide,  $\text{Fe}_3\text{C}$ , in the film. Most authors believe that the film acts as a diffusion barrier. Other points of views will be discussed later.

The above authors have noticed a temperature effect for corrosion with a protective film. However, the nature of the temperature dependence is a point of division among the authors. Ikeda et al. (1984) reported three distinct temperature regions corresponding to different mechanisms. Below  $60^\circ\text{C}$ , a small amount of soft and nonadhesive iron carbonate forms on the surface. The surface is smooth and corrosion attack is homogeneous. In the vicinity of  $100^\circ\text{C}$ , where the corrosion rate is maximum under their

experimental conditions, the corrosion product was a coarse, porous thick film of  $\text{FeCO}_3$  on the substrate. As later explained by Xia et al. (1989), a porous layer of corrosion product can screen some sites on the metal surface from the attack by  $\text{HCO}_3^-$  ions. However, some sites are exposed to the corrosion medium, hence, galvanic couples result. In the temperature range above  $150^\circ\text{C}$ , the corrosion product is thin and adhesive, so that the corrosion rate is lower. Hausler (1984), however, showed that the corrosion rate is higher at  $60^\circ\text{C}$  than that at both  $90$  and  $120^\circ\text{C}$ . Valand and Sjøwall (1989) observed that below  $80^\circ\text{C}$  the corrosion rate obeys Arrhenius' law with an apparent activation energy of  $6.5$  kcal/mol for the corrosion process. Choi et al. (1989) indicated that the corrosion rate is at its maximum at  $70^\circ\text{C}$  and at  $90^\circ\text{C}$  the corrosion rate is lower than that at  $70^\circ\text{C}$  by a factor of 5. These differences from different authors have not been satisfactorily explained. One of the possible explanations is that the flow and mass transfer rates are different for the different researchers.

The elementary step of the corrosion process is not very clear at this stage. As repeatedly pointed out previously, most authors tried to explain the retardation of the corrosion rate by the corrosion product layer forming a diffusion resistance. From another point of view, Hausler (1984) has proposed that corrosion with a

solid product film occurs by the mechanism of iron transport through a semiconductor film. However, it is very difficult to verify this mechanism quantitatively since too many parameters are unknown for the  $\text{FeCO}_3$  film to be modelled as a semiconductor film.

### Mechanisms of Mass Transfer in the Corrosion Processes

In the corrosion processes, mass transfer plays an important role. Although many publications deal with the relationship between the mass transfer and the corrosion rate, the basic mechanisms are far from being completely understood.

Pouson (1983) reviewed various mass transfer correlations between the metal and electrolyte solutions, including various flow geometries. But all these correlations are from single phase laminar or turbulent flow including the well-known Chilton-Colburn analogy. In these correlations, the effect of wall roughness on the corrosion rate is not included explicitly. However, the effect of wall roughness on the corrosion rate has long been realized to be an important factor.

Ross and Badhwar (1965) have investigated the influence of wall roughness on the corrosion rate. They found that a cavity shaped roughness with depth about 0.6 of its diameter was particularly conducive to faster

corrosion rates. This shape factor has not been explained satisfactorily.

Mahato and Shemilt (1968) in their studies of corrosion of iron by natural water confirmed the theoretical model of Levich (1962). If Levich's model can fit experimental data it would mean that the wall mass transfer in the corrosion processes is mainly due to the turbulent eddies with a size about the height of wall roughness. This conclusion can be clearly seen from Levich's theoretical analysis. When Levich's theory is applied to corrosion processes, one difficulty is to characterize the wall roughness.

Mahato et al. (1980) realized this problem and developed a more sophisticated mass transfer model for corrosion of steel pipe in aerated water. In this model, various factors have been taken into accounts, including build-up of corrosion product, growth of surface roughness, changing physicochemical properties of corrosion products and changing hydrodynamic conditions. The general mathematical model proposed fitted experimental data well. However, from the view point of corrosion rate prediction this model is quite backwards because this model needs the overall corrosion rate as a necessary input. Notwithstanding this limitation, the model does predict values for the porosity of the corrosion product and the friction factor which is in good agreement with

experimental data. They concluded that mass transfer in the damped turbulent boundary layer controls the overall mass transfer process for the time and flow rate range investigated. This is consistent with Levich's theory.

Various results have been reported about the influence of mass transfer on the corrosion rate. Eriksrud and Søntvedt (1984) found that the corrosion rate in CO<sub>2</sub> solutions is proportional to a power of 0.3 on the Reynolds number. This probably means that both mass transfer and surface reaction have some influences on the corrosion rate. This point can also be deduced from the work by Tewari and Campbell (1979), who have studied the corrosion rate of carbon steel in 0.1 MPa H<sub>2</sub>S aqueous solutions and found both mass transfer and dissolving FeSH<sup>+</sup> contributing to the corrosion rate. Further evidence that the corrosion rate is determined by both surface reaction and mass transfer can be seen from other research results (Videm and Dugstand 1987, Postlethwaite and Lotz 1988) similar to those mentioned.

Still another mechanism has been proposed for the mass transfer in the corrosion process by Sato (1989). He proposed that a porous precipitated film of corrosion product is like an ion selective membrane. The properties of this membrane depend upon its "fixed charge," which is defined as an immobile electric charge attached to the porous wall of the product film. Depending on its fixed

charge and the mobile cation and anion concentrations, the film is termed anion-selective, cation-selective, or a bipolar membrane. According to this mechanism, the mass transfer is controlled by the properties of the film, which only selectively allow anions or cations to pass through the film. He further reasoned that the anion-selective film accelerates the corrosion rate and the cation-selective film depresses the corrosion rate. A bipolar precipitate film, if anodically polarized, undergoes deprotonation and turns into a passive film. Conceptually, this mechanism can explain some corrosion phenomena well, qualitatively. However, the means of determining the kind of ion-selective film (membrane) that would be formed on the surface under given conditions is not yet available. Furthermore, quantitative characterization of the film is also a problem to be solved. Therefore, a lot of work must still be done before this mechanism can be used to predict the corrosion rate.

In summary, the mechanisms of downhole gas well corrosion can be categorized as surface reaction and mass transfer with or without formation of a product film. Probably both  $H_2S$  and  $CO_2$  molecules take part in the surface electrochemical reactions. Under certain conditions  $HCO_3^-$  and  $HS^-$  may also be a part of the cathodic reactions. The corrosion product formed on the surface may have some protective effect by acting either as a diffusion



barrier or as a semiconductor film, the latter of which is more difficult to describe quantitatively. The eddies with the size of the height of the surface roughness make the main contribution to the mass transfer near the wall. Corrosion rate is not totally controlled by convective mass transfer under most circumstances. The corrosion product film may be modelled as an ion-selective membrane; but much work needs to be done before one can quantitatively describe the mass transfer process through this film.

#### Modeling Downhole Corrosion

Crolet and Bonis (1984) have commented on the importance of prediction of downhole corrosion and its economic impact. However, using a mathematical model to predict downhole corrosion is a relatively new area. In this section, some related work will be discussed.

Robertson and Erbar (1988) made an attempt to simulate downhole corrosion. In this research, a computer model has been developed that can be used to predict downhole pressure and temperature profiles and phase behavior. Therefore, the corrosion engineer can check to see whether a water rich liquid phase exists and what two-phase flow regime exists for the specific downhole conditions. Similar research has also been done by Reinhart and Powell (1988). This model is almost the same as that of Robertson and Erbar (1988). But in Reinhardt and Powell's model both

temperature and pressure profiles are assumed to be linear and the downhole two-phase flow patterns are not calculated. Neither model calculated the downhole corrosion rate.

Later, Fang et al. (1989) developed a model that can be used to calculate downhole flow patterns, phase behavior and the single pitting propagation rate. However, in their pitting propagation model only  $Fe^{++}$  ion mass transfer from pit to bulk liquid is considered. This model did not provide any criteria for the conditions of initiating pitting corrosion. Therefore, it is an oversimplified model.

Liu and Erbar (1990) proposed another model. In this model, the hydrogen ion is assumed to be key the corrosive species in  $H_2S$  and  $CO_2$  aqueous medium. The hydrogen ion concentration is calculated through dissociation equilibrium at downhole temperatures and pressures. The model can predict the uniform corrosion rate in systems without a protective film. Although this is also an oversimplified model, it really made the first attempt to include fluid dynamics, mass transfer, and surface reaction mechanisms in a single model.

From this survey of modeling of downhole corrosion, it can be seen that prediction of downhole corrosion is in a very early stage of development. Any practical model has to take downhole fluid flow, mass transfer and surface

electrochemical reactions into account.

#### Summary of the Literature Survey

1). Complete understanding of downhole corrosion phenomena has not been achieved.

2). Many researchers have investigated the mechanisms of downhole corrosion. Surface electrochemical reactions involve corrosive species ( $H_2S$  and  $CO_2$ ) adsorption and charge transfer.

3). More quantitative experimental measurements are needed concerning the transport processes through the corrosion product film.

4). A better model is needed to predict downhole corrosion. Since most of the experimental evidence shows that downhole corrosion processes have both mass transfer and surface reaction contributions, a practical model has to take these factors into account.

## CHAPTER III

### MODEL DESCRIPTION

#### Physical Model

The system downhole in a gas well can be physically described by examining the corrosion processes as follows: Natural gas with or without formation water leaves the reservoir and enters the tubing at high temperature and pressure. Owing to the temperature and pressure gradients in the well, water condensation may occur at some upper position in the well. Under most circumstances, gas flow rates are relatively high. Therefore, most of the gas wells are in annular two-phase flow. Some of these wells are in slug flow, which is more complicated than annular flow in terms of the corrosion rate prediction. For an annular flow gas well, the flow pattern is shown in Figure 1.

As shown in Figure 1, the gas flows in the center part of the tubing and the liquid moves along the tube wall as a thin film. The gas shear stress at the gas-liquid interface must be strong enough to overcome the wall shear stress and gravitational effect. When the gas shear is stronger than that the film can absorb, some liquid in the

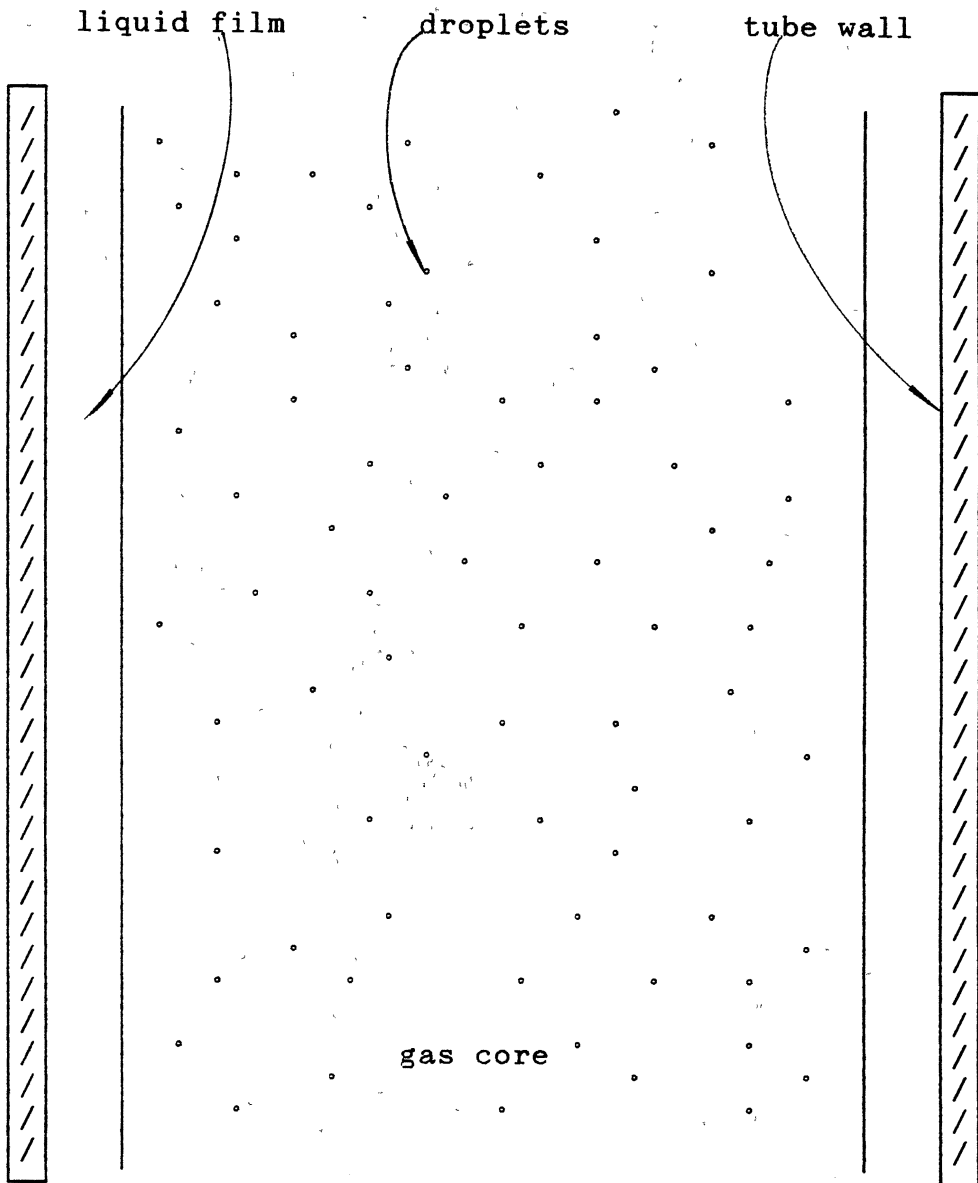


Figure 1. Schematic Diagram of Downhole Annular Two-Phase Gas-Liquid Flow

film is entrained in the gas as droplets. Once droplets are entrained, some of them will also be redeposited onto the film downstream until a dynamic equilibrium is reached.

The corrosive gases ( $H_2S$  and  $CO_2$ ) will dissolve into the liquid film. The dissolved gases will disassociate into their corresponding ions, such as  $HS^-$ ,  $HCO_3^-$ ,  $S^{2-}$  and  $CO_3^{2-}$ . These ions together with the dissolved gas species are transported to the solid-liquid interface, where corrosion may occur. At the initial stage of corrosion, a fast wall dissolution reaction occurs. A part of the dissolved ferrous ions is transported into the liquid film. Some portion of the ferrous ions will be deposited on the wall through either a direct formation reaction or precipitation. The corrosion products formed on the wall will retard the corrosion rates and increase wall roughness.

Based on the above description of the system, the following assumptions are made for the system.

- (1). Equilibrium is achieved at the gas and liquid interface, including the ion disassociation reactions.
- (2). Steady state is reached.
- (3). Electroneutrality holds through the whole liquid film and liquid and solid interface.
- (4). All the inorganic ions from formation water do not take part in the corrosion reactions but have influence on the electroneutrality.

(5). For those wells where the two-phase flow is in the slug flow region the corrosion rate calculation can be made based on the annular flow model.

(6). The solution can be assumed to be dilute.

Assumption (1) can be justified from the experimental results of Jagota et al. (1973), who have studied the mass transfer at the gas and liquid interface in two-phase annular flow and found that equilibrium at the interface is reached in a fairly short distance from the inlet (about 3 feet). Assumption (2) is true considering that the main time concern in the prediction of downhole corrosion is in terms of several years of time. Assumption (3) has been reasonably justified by some others (Newman 1973).

Assumption (4) is not easily justified since whether chloride directly takes part in the interface reactions is not very clear. However, the main concern of this model is to predict the uniform corrosion rates. This effect probably is not as prominent as in the case of pitting corrosion. Assumption (5) can not reasonably be justified since it has been found that the wall shear stress is much higher under slug flow than under annular flow (Johnson et al. 1991) and corrosion rates are generally higher in this flow regime (Eriksrud and Sontvedt 1984, Videm and Dugstad 1987). Although this increase in the corrosion rate by flow is much more related to localized corrosion rates, its influence for the uniform corrosion rate is not very clear.

This assumption can only be removed through further study. Assumption (6) is reasonable since the ionic strength of gas well brines is generally much less than 1.0.

Based on the assumptions and descriptions of the system, the corrosion processes probably can be modelled as a three layer model as shown in Figure 2.

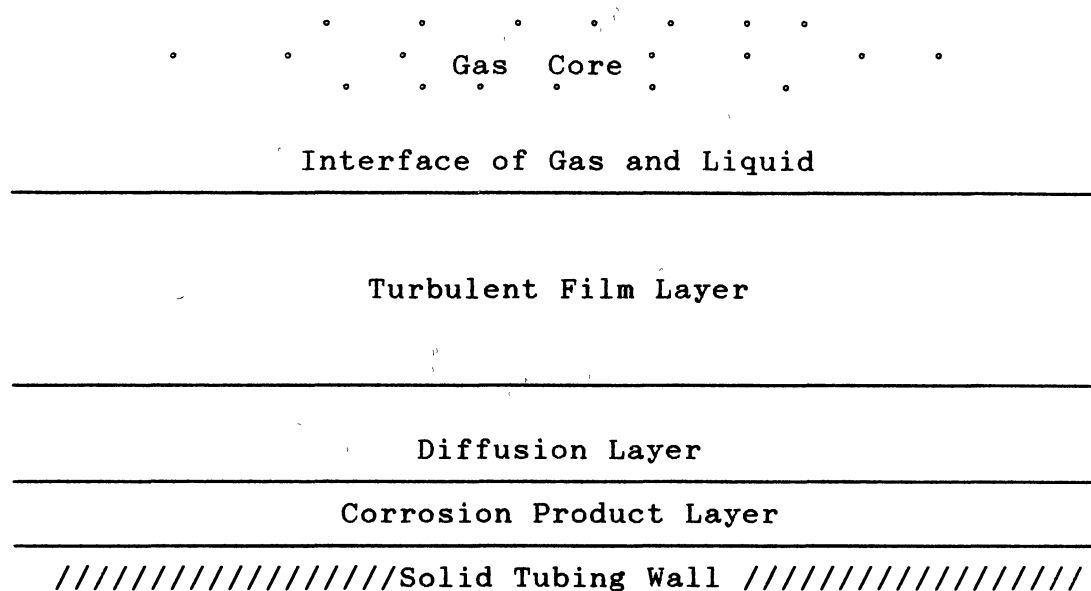


Figure 2. Composite Structure of Corrosion Processes for Annular Two Phase Flow.

Corrosive species are transported through the turbulent liquid film layer, where turbulent mass transfer is important. This layer in the model includes most of the



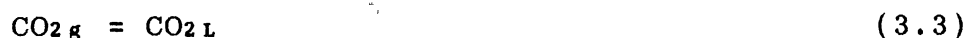
viscous sublayer. Further the wall roughness will also have an influence on the mass transfer in this layer as is discussed later.

In the diffusion layer, the mass transfer is dominated by diffusion and ion migration. At the initial stage of corrosion no corrosion product is formed on the metal wall. Therefore, the corrosion reaction occurring on the wall is the boundary of this layer. If there is corrosion product buildup on the wall, the corrosive ions will diffuse and migrate through the diffusion layer into the corrosion product layer. The ferrous ions from the wall will diffuse and migrate in the opposite direction.

### Model Formulations

#### The Interface of the Gas and Liquid

The equilibrium relations at the interface of the gas and liquid can be summarized as follows:





From these equilibrium relations, the concentration of each species can be calculated through the necessary conditions for equilibrium.

For the molecular solute, equilibrium between the vapor phase and the liquid phase is given by

$$y_1 f_1 P = m_1 \phi_1 H \quad (3.9)$$

For disassociation reactions, we have

$$K_{1, \text{H}_2\text{S}} = \frac{[\text{HS}^-][\text{H}^+]}{[\text{H}_2\text{S}]} \quad (3.10)$$

$$K_{2, \text{H}_2\text{S}} = \frac{[\text{S}^{= }][\text{H}^+]}{[\text{HS}^-]} \quad (3.11)$$

$$K_{1, \text{CO}_2} = \frac{[\text{HCO}_3^-][\text{H}^+]}{[\text{H}_2\text{CO}_3]} \quad (3.12)$$

$$K_{2, \text{CO}_2} = \frac{[\text{CO}_3^{2-}][\text{H}^+]}{[\text{HCO}_3^-]} \quad (3.13)$$

$$K_w = \frac{[\text{H}^+][\text{OH}^-]}{[\text{H}_2\text{O}]} \quad (3.14)$$

The electroneutrality relation is

$$\sum_i Z_i m_i = 0 \quad (3.15)$$

This equilibrium system contains 12 independent variables:  $\text{H}_2\text{S}_L$ ,  $\text{H}_2\text{CO}_3$ ,  $\text{HS}^-$ ,  $\text{HCO}_3^-$ ,  $\text{S}^{2-}$ ,  $\text{CO}_3^{2-}$ ,  $\text{H}_2\text{O}$ ,  $\text{H}^+$ ,  $\text{OH}^-$ ,  $y_{\text{H}_2\text{S}}$ ,  $y_{\text{CO}_2}$  and the total amount of vapor  $V$ . While equations (3.9), which represent three vapor-liquid equilibria ( $i = \text{H}_2\text{S}$ ,  $\text{CO}_2$ , and  $\text{H}_2\text{O}$ ), through (3.15) give nine relations, we need three additional equations. These are the element balances.

Sulfur balance

$$\text{H}_2\text{S}(\text{in feed}) = y_{\text{H}_2\text{S}} V + (\text{H}_2\text{S}_L + \text{HS}^- + \text{S}^{2-}) \quad (3.16)$$

Carbon balance

$$\text{CO}_2(\text{in feed}) = y_{\text{CO}_2} V + (\text{H}_2\text{CO}_3 + \text{HCO}_3^- + \text{CO}_3^{2-}) \quad (3.17)$$

Hydrogen balance

$$2(\text{H}_2\text{O} + \text{H}_2\text{S})(\text{in feed}) = 2(y_{\text{H}_2\text{S}} + y_{\text{H}_2\text{O}})V + 2\text{H}_2\text{O} + 2\text{H}_2\text{S} \\ + (\text{HS}^- + \text{H}^+ + \text{OH}^- + \text{HCO}_3^-) \quad (3.18)$$

All the equilibrium and Henry's constants for the system are taken from the work by Edwards et al. (1978) and Kawazuishi and Prausnitz (1987). The equilibrium constants are expressed as

$$\ln K_i = A_1/T + A_2 \ln T + A_3 T + A_4 \quad (3.19)$$

The constants  $A_j$  ( $j=1,2,3,4$ ) are given in Table I.

TABLE I  
TEMPERATURE COEFFICIENTS FOR  
EQUILIBRIUM CONSTANTS

Elec- trolyte	$A_1$	$A_2$	$A_3$	$A_4$	Range of Validity °C
CO <sub>2</sub>	-12092.1	-36.7816	0.0	235.482	0-225
H <sub>2</sub> S	-18034.7	-78.0719	0.092	461.716	0-275
HCO <sub>3</sub> <sup>-</sup>	-12431.7	-35.4819	0.0	220.067	0-225
HS <sup>-</sup>	-406.004	33.8889	-0.054	-214.559	0-225
H <sub>2</sub> O	-13445.9	-22.4773	0.0	140.932	0-225

The Henry's constants are given by

$$\ln H_1 = B_1/T + B_2 \ln T + B_3 T + B_4 \quad (3.20)$$

with the constants  $B_j$  ( $j=1,2,3,4$ ) given in Table II.

TABLE II  
TEMPERATURE COEFFICIENTS FOR  
HENRY'S CONSTANTS

Electrolyte	B1	B2	B3	B4	Range of Validity °C
CO <sub>2</sub>	-6789.04	-11.4519	-0.010454	94.4914	0-250
H <sub>2</sub> S	-13236.8	-55.0551	0.0595651	342.595	0-150

The fugacity coefficients for the gas phase are calculated by the SRK equation of state. The activity coefficients for the system are adopted from the work by Kerr (1980) with the expression,

$$\log \phi_i = A_{\phi} Z_i^2 \left[ -I^{1/2} / (1+I^{1/2}) + b_i I \right] \quad (3.21)$$

The Debye-Huckel parameter,  $A_\phi$ , for aqueous electrolyte systems is calculated by the following expression

$$\begin{aligned}
 A_\phi = & 0.377388 + 2.5368E-4t + 1.7892E-5t^2 - 3.48184E-7t^3 \\
 & + 4.24739E-9t^4 - 2.87647E-11t^5 + 1.09781E-13t^6 \\
 & - 2.20446E-16t^7 + 1.82433E-19t^8 \quad (3.22)
 \end{aligned}$$

obtained from data correlation of Debye-Huckel parameter values reported by Bradley and Pitzer (1979). This correlation is numerically not very different from the one by Chen et al. (1982) from the same set of data but this polynomial fitting is easier to use than that by Chen et al. (1982).

The values for  $b_i$  are all 0.3 except for a few species, which are listed in Table III.

TABLE III  
 VALUE OF  $b_i$  FOR SOME SPECIES  
 IN EQUATION (3.21)

Species	H <sup>+</sup>	Na <sup>+</sup>	Ca <sup>++</sup>	Cl <sup>-</sup>	CO <sub>3</sub> <sup>=</sup>	HCO <sub>3</sub> <sup>-</sup>	HS <sup>-</sup>
$b_i$	0.4	0.1	0.1	0.0	0.0	0.0	0.0

And ion strength is defined as

$$I = 0.5 \sum_i m_i Z_i^2 \quad (3.23)$$

Equation (3.21) can be used for ion strength up to 1M. For almost all the downhole brines, this is a valid range.

The activity coefficients of uncharged species can be calculated using the expression (Kerr 1980)

$$\log \phi_i = 0.076I \quad (3.24)$$

If the system contains some other inorganic species, such as  $\text{Na}^+$ ,  $\text{Ca}^{++}$ ,  $\text{Cl}^-$ , the only influence of these species on the equilibrium calculation is electroneutrality under the assumption of the model. However, if the solubility product of  $\text{CaCO}_3$  is reached, another equilibrium relation is involved.

$$K_{sp, \text{CaCO}_3} = [\text{Ca}^{++}] [\text{CO}_3^{--}] \quad (3.25)$$

The value of  $K_{sp, \text{CaCO}_3}$  is calculated by the following expression

$$\ln K_{sp, \text{CaCO}_3} = -65.92499 - 0.09288796T + 14.62471 \ln T - 2748.51/T \quad (3.26)$$

obtained from data correlation reported by Ellis (1959), Segnit et al. (1962), Langmuir (1968), Jacobson and Lanmuir (1974), Plummer and Busenberg (1982). The correlation has a valid temperature range of 0-300 °C and CO<sub>2</sub> pressure up to 60 bar.

With the equilibrium relations listed above the concentration of each species at the interface of gas and liquid can be calculated. The results will be used for the boundary conditions for the mass transfer calculation.

#### Mass Transfer Through Turbulent

#### Film Layer

As mentioned in the literature survey, although a lot of work has been done in the area of mass transfer we have found no simple correlation that can be used in two-phase annular flow mass transfer though the turbulent layer towards the wall. In the mass transfer research literature in annular two-phase gas-liquid flow much attention is paid to the gas and liquid interface (Jagota et al. 1973, Kasturi, et al. 1974, McCready and Hanratty 1985, McCready et al. 1985, Back and McCready 1988, Caussade et al. 1990, Chekhovich and Pecherkin 1987-1988). Wasden and Dukler (1990) have made a study of mass transfer from the wall for free falling wavy films. In this model, no interfacial shear stress has been considered. Therefore, it seems necessary to develop a model that considers the interfacial



shear and wall roughness in the corrosion processes. Since the mechanism of the mass transfer process under consideration is not very clear to the author the model must be speculative and can only be good within a reasonable theoretical framework.

The momentum equation for a one dimensional liquid film can be written as

$$-\frac{dp}{dz} + \rho_L g + \frac{1}{r} \frac{d}{dr} (r \tau) = 0 \quad (3.27)$$

with the boundary condition:

at the wall

$$r = R \quad \tau = \tau_w \quad (3.28)$$

Integrating equation (3.27) with boundary condition (3.28) and using the gas-liquid interface condition ( $r = r_i$ ,  $\tau = \tau_i$ ) to remove the pressure gradient and gravitation term, we have

$$\frac{\tau}{\tau_w} = 1 - \left( 1 - \frac{\tau_i}{\tau_w} \right) \eta \quad (3.29)$$

where

$$\eta = \frac{y}{\delta} \quad (3.30)$$

On the other hand, the shear stress can also be expressed as

$$\tau = (\mu_L + \mu_t) \frac{dU}{dy} \quad (3.31)$$

In the following we use a method similar to that of Vulchanov and Zimparov (1989) for single phase flow to derive a friction factor expression for two phase film flow. Equation (3.31) can be made dimensionless.

$$\frac{\tau}{\tau_w} = \frac{1}{\delta^+} \left( 1 + \frac{v_t}{v_L} \right) \frac{dU^+}{d\eta} \quad (3.32)$$

where,

$$\delta^+ = \frac{\delta u^*}{v_L} \quad (3.33)$$

$$U^+ = U/u^* \quad (3.34)$$

$$u^* = (\tau_w / \rho_L)^{1/2} \quad (3.35)$$

According to Prandtl mixing-length theory the eddy viscosity can be expressed as

$$\frac{v_t}{v_L} = \delta^+ (I_m^+ / \delta^+)^2 \frac{dU^+}{d\eta} \quad (3.36)$$

where  $I_m$  is mixing-length and

$$I_{\eta}^{\dagger} = \frac{I_{\eta} u^{\dagger}}{v_L} \quad (3.37)$$

Strong interfacial shear and very thin thickness probably makes the liquid film much like a damped turbulent layer. Therefore, the expression for mixing length by Van Driest (Hinze 1975) can be used.

$$I_m = 0.4y[1 - \exp(-y^{\dagger}/26)] \quad (3.38)$$

or

$$I_{\eta}^{\dagger}/\delta^{\dagger} = 0.4 \eta [1 - \exp(-\eta\delta^{\dagger}/26)] \quad (3.39)$$

The above treatment of the film layer does not consider the wall roughness. To include wall roughness the approach of Rotta will be used. Cebici and Smith (1974) gave a detailed review of this method. The effect of roughness is considered to be equivalent to a change in the velocity jump across the viscous sublayer. It can be represented by a shift of smooth-flow velocity profile. For rough flow, the reference plane (wall) is shifted by an amount  $y'$ , and the reference plane moves with the velocity  $U'$  in a direction opposite to that of the main flow. Here dimensionless  $\eta'$  is expressed as (Cebici and Smith 1974).

$$\eta' = 0.9[(k_s^{\dagger})^{0.5} - k_s^{\dagger} \exp(-k_s^{\dagger}/6)]/\delta^{\dagger} \quad (3.40)$$

It is noted that the wall roughness of corrosion product may not be the same as the sand-type roughness. But as there are no characterizations available for corrosion wall roughness the sand-type correlation is used in this model.

Combination of equations (3.29), (3.31), (3.34) and (3.38), after some manipulation, gives

$$\frac{dU^+}{d\eta} = \frac{2 \delta^+ [1 - (1 - \tau_i / \tau_w)(\eta + \eta')]}{1 + \{1 + 4(\delta^+)^2 [1 - (1 - \tau_i / \tau_w)(\eta + \eta')] (I_n^+ / \delta^+)^2\}^{1/2}} \quad (3.41)$$

with boundary condition

$$\eta = \delta_1 \quad U^+ \approx 0 \quad (3.42)$$

where  $\delta_1$  is the thickness of the diffusion layer.

From the definition of the friction factor, one has

$$f = \frac{2 \tau_w}{\rho_L U_{av}^2} \quad (3.43)$$

with

$$U_{av} = \frac{1}{\pi(R^2 - r_i^2)} \int_{r_i}^R 2\pi r U dr$$

$$\approx \int_0^1 (1 - \eta) U \, d\eta \quad (3.44)$$

Substitution of equation (3.42) into (3.41) gives

$$f = \frac{2}{\left[ \int_0^1 (1 - \eta) U^+ \, d\eta \right]^2} \quad (3.45)$$

Once  $U^+$  is calculated from equation (3.39) with boundary condition (3.40) by numerical integration of the initial value problem, the friction factor can be calculated from equation (3.43).

For the mass transfer calculation we can write the total mass flux as

$$N_1 = (D_1 + \epsilon_D) \frac{dC_1}{dy} \quad (3.46)$$

In terms of dimensionless variables, we have

$$Sh = \frac{K_L \delta}{D_1} = Re_f \left( \frac{f}{2} \right)^{1/2} Sc K^+ \quad (3.47)$$

where,

$$K^+ = \frac{K_L}{u^*} \quad (3.48)$$

In the corrosion process, the electrolyte has a Schmidt number ranging from 500 to 1500. This means that the eddy diffusivity for mass transfer varies with  $(y^+)^3$  in almost all parts of the boundary layer for single phase flow (Mizushima et al. 1971). For the liquid film flow it is probably also true. Therefore, we have

$$\frac{\epsilon_D}{\nu_L} = A (y^+)^3 \quad (3.49)$$

Substituting equation (3.46) into (3.44) with assumption of constant mass flux we have

$$\begin{aligned} K^+ &= 1 / \int_{\delta_1^+}^{\delta^+} \frac{dy^+}{1/Sc + A(y^+)^3} \\ &\approx 1 / \int_0^{\delta^+} \frac{dy^+}{1/Sc + A(y^+)^3} \\ &= 6 A^{1/3} Sc^{-2/3} \left[ \frac{\sqrt{3}\pi}{3} + 2\sqrt{3} \arctg \frac{2\delta^+ - (ASc)^{-1/3}}{\sqrt{3}(ASc)^{-1/3}} \right. \\ &\quad \left. + \ln \frac{[(ASc)^{-1/3} + (\delta^+)]^2}{(ASc)^{-2/3} - (ASc)^{-1/3}\delta^+ + (\delta^+)^2} \right]^{-1} \quad (3.50) \end{aligned}$$

The coefficient, A, has a value  $3.2-5.2 \times 10^{-4}$  (Lin et al. 1953, Mizushima et al. 1971, Granville 1990) for single phase turbulent boundary layer flow. For two-phase flow, as mentioned before, the whole liquid film can be treated as a damping turbulent layer. Hence, a medium value of  $A = 4.5 \times 10^{-4}$  is taken.

Inserting equations (3.47) and (3.43) into (3.45), one can calculate the mass transfer coefficients with the known parameters. The parameters in the above equations involve  $\tau_i$ ,  $\tau_w$ ,  $\delta$  and  $k_s^+$ . Their estimations will be discussed in the following.

The interfacial shear stress can be calculated from the following expression (Bergles et al. 1981).

$$\tau_i = 1/2 f_{ti} \rho_c U_c^2 \quad (3.51)$$

where,

$$f_{ti} = 0.079 Re_c^{-1/4} \left( 1 + 360 \frac{\delta^+}{D^+} \right) \quad (3.52)$$

$$\rho_c = \rho_g \left( \frac{W_g + W_{LB}}{W_g} \right) \quad (3.53)$$

$$U_c = \frac{4(W_g + W_{LB})}{\pi \rho_c (D-2\delta)^2} \quad (3.54)$$

The film thickness is calculated by the correlation of Henstock and Hanratty (1976) with the expression

$$\frac{\delta}{D} = \frac{6.59F_o}{(1 + 1400F_o)^{1/2}} \quad (3.55)$$

where,

$$F_o = \frac{\beta}{Re_g^{0.9}} \frac{v_L}{v_g} \left[ \frac{\rho_L}{\rho_g} \right]^{0.5} \quad (3.56)$$

and

$$\beta = [(0.707Re_f^{1/2})^{2.5} + (0.0379Re_f^{0.9})^{2.5}]^{0.4} \quad (3.57)$$

A method for the estimation of wall roughness is not available in the literature. Although for the corrosion of steel pipe in single phase flow, Mahato et al. (1980) gave a correlation for estimating wall roughness, this correlation needs the overall corrosion rate as an input. Hence, it can not be used for the purpose of this model. For annular flow, the film thickness is very thin. If we consider interfacial wavy flow the maximum possible height of wall roughness can only be the thickness of the continuous layer. Furthermore, if the fluctuation of the thickness of the continuous layer is considered, the wall roughness can never reach this maximum height. Based on



the above reasoning, it is assumed that the wall roughness be half of the continuous layer thickness. Using the correlation for the continuous layer thickness ( Dobran 1983), We have

$$k_s^+ = .70 D^+ N_1^{0.433} Re_c^{-1.35} \quad (3.58)$$

where,

$$N_1 = [gD^3 \rho_L (\rho_L - \rho_g) / \mu_L ]^{1/2} \quad (3.59)$$

By knowing the above parameters  $\tau_w$  can be calculated through the momentum balance for the liquid film with the following expression

$$\tau_w = \tau_i + (dp/dz - \rho_L) \delta / 2 \quad (3.60)$$

With the above parameters estimated mass transfer through the turbulent layer can be calculated.

### Mass Transfer and Ion Migration

#### Through Diffusion Layer

In the corrosion processes for the multicomponent systems with which we are concerned, surface electrochemical reactions will set up an electric field. We can define a very thin layer called the diffusion layer

(Newman 1973) in which diffusion and ion migration are dominant. This definition is quite arbitrary since we can also put this layer into the turbulent mass transfer layer. But for multicomponent systems the mathematical treatment is intractable because of the highly nonlinear form in both the governing equations and boundary conditions. If one divides the liquid film layer into two layers as was done in this model, the system will not be very difficult to handle. According to the assumption for the diffusion layer, the mass balances in this layer can be written as

$$D_i \frac{d^2 C_i}{dy^2} + Z_i u_i F \frac{d}{dy} \left( C_i \frac{d\Phi}{dy} \right) = 0 \quad (3.61)$$

where,

$$u_i = \frac{D_i}{R T} \quad (3.62)$$

with boundary conditions:

At  $y = 0$ , there are two types of boundary conditions. One is a so-called active wall, at which no corrosion product has formed. Another type occurs when corrosion product has formed on the wall. In the former case,

for nonreactive species,

$$D_i \frac{dC_i}{dy} + Z_i u_i F C_i \frac{d\Phi}{dy} = 0 \quad (3.63)$$

and for reactive species

$$D_1 \frac{dC_1}{dy} + Z_1 u_1 F C_1 \frac{d\Phi}{dy} = \frac{I_1}{n F} \quad (3.64)$$

In the later case,

$$C_1 = C_{1s} \quad (3.65)$$

At  $y = \delta_1$

$$C_1 = C_{i1} \quad (3.66)$$

Equation (3.58) with boundary conditions (3.60) - (3.61) or (3.62) and (3.63) are nonlinear equations with nonlinear or linear boundary conditions. No analytical solution is known. Therefore, the finite difference method (FDM) will be used. Before FDM is used the system equations and its boundary conditions are quasilinearized. The detailed computational method will be discussed later.

### Mass Transfer Through the Corrosion

#### Product Layer

The mass transfer through the corrosion product layer can be formulated as diffusion through a porous medium. Therefore, the governing equation will be the same as expressed in equation (3.58) by using effective diffusivity instead of the diffusion coefficients. The boundary conditions (3.60) and (3.61) can also be used by making the

same modifications.

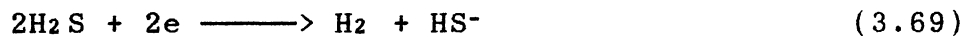
### Kinetics of Surface Reactions

The mechanisms of surface reactions for downhole corrosion, as discussed in the literature survey are not fully understood. Based on the literature (De Waard and Milliams 1975, Ogundele and White 1986, 1987, Morris et al., 1980 and Wieckowski et al., 1983, Wikjord et al., 1980) the following reactions are assumed to occur on the metal surface for this model.

Anode



Cathode



According to the electrochemical theory of corrosion (Evans 1960), the corrosion process takes place at a mixed potential,  $E_{\text{corr}}$ . It is presumed that the Butler-Volmer expression (Newman, 1973, p17.) can be applied to the kinetics of system reactions. The following expressions

are used in the calculation of reaction current densities:

For anodic reaction (3.64)

$$i_a = i_{a0} \exp(\alpha_a F \eta_a / RT) \quad (3.70)$$

where,

$$\eta_a = E_{\text{corr}} - E_{e,M} \quad (3.71)$$

and where  $i_{a0}$ , exchange current density, is a function of temperature and some other parameters. At 25°C, Bockris et al. (1961) reported that  $i_{a0}$  has values ranging from  $1.1 \times 10^{-5}$  to  $3 \times 10^{-8}$  A/cm<sup>2</sup> depending upon pH and ferrous ion concentrations. Gray et al. (1989) gave a value of  $i_{a0}$   $5.0 \times 10^{-8}$  A/cm<sup>2</sup> at pH 4. Ogundele and White (1986) reported  $1 \times 10^{-7}$  A/cm<sup>2</sup> for this reaction. On the average, all these reported data give a value of  $i_{a0} = 2.0 \times 10^{-7}$  A/cm<sup>2</sup> at 25°C, which was used in this model. For the anodic reaction, the equilibrium potential can be derived from the Fe<sup>++</sup>/Fe electrode reaction which has an equilibrium potential (Bard et al. 1985) of

$$E_{e,M} = -0.44 + \frac{RT}{2F} \ln[\text{Fe}^{++}] \quad (3.72)$$

For the particular case involving an H<sub>2</sub>S and/or CO<sub>2</sub> solution, the activity of Fe<sup>++</sup> is related to the following

reactions:

reactions (3.1)-(3.8) and (3.25) in addition to



with

$$K_{sp, \text{FeCO}_3} = [\text{Fe}^{++}] [\text{CO}_3^-] \quad (3.75)$$

$$K_{sp, \text{FeS}} = [\text{Fe}^{++}] [\text{S}^-] \quad (3.76)$$

When all the equilibrium constants are known the equilibrium potential can be calculated.

For cathodic reactions the corrosion current is expressed as:

For reaction (3.65)

$$i_{c1} = i_{c10} \exp(\alpha_{c1} F \eta_c / RT) \quad (3.77)$$

where,

$$\eta_c = E_{\text{corr}} - E_{e,80} \quad (3.78)$$

with a value of  $i_{c10}$  taken as  $4.0 \times 10^{-6}$  A/cm<sup>2</sup> (Gray et al. 1986) at 25°C and activation energy as 10.7 kcal/mol (De Waard and Milliams 1975).

For reaction (3.66)

$$i_{c2} = i_{c20} \exp(\alpha_{c2} F \eta_c / RT) \quad (3.79)$$

with the value of  $i_{c20}$  taken as  $8.96 \times 10^{-6}$  A/cm<sup>2</sup> (Morris et al. 1980) at 25°C and activation energy as 18.4 kcal/mol. (Tewari and Campbell 1979).

The equilibrium potential at the cathode can be calculated in the same way as that at the anode.

Another important parameter in the calculations of surface kinetics is the corrosion potential of the system. In the literature, no data have been found that cover the system conditions and species downhole. For a corrosion system, since there is no net current flow, the total cathodic current must be equal to the total anodic current. If it is assumed that cathodic and anodic reactions have equal surface areas over which these reactions occur, the following relation is true

$$i_a = i_{c1} + i_{c2} \quad (3.80)$$

By knowing  $E_{e,m}$  and  $E_{e,so}$  and the other parameters discussed above,  $E_{corr}$  can be calculated through solving equations (3.67), (3.74) and (3.76) with the relation (3.77). Of course, all the reasonable values of  $E_{corr}$  must be located between the anodic and cathodic equilibrium potentials. The assumption of equal reaction areas for both anodic and cathodic reactions is not a very good one.

However, it is the only way known to the author to obtain the  $E_{\text{corr}}$  without experimental data. For the uniform corrosion considered here this assumption is a better approximation than it would be for localized corrosion, in which the anodic reaction area is much less than the cathodic reaction area.



## CHAPTER IV

### NUMERICAL SOLUTIONS OF THE SYSTEM MODEL

#### Solution of Gas and Liquid Interface

System model equations (3.9) through (3.18) with the additional requirement

$$y_{H_2O} + y_{H_2S} + y_{CO_2} = 1 \quad (4.1)$$

contains 13 nonlinear equations, which can be solved by the Newton-Raphson method. This method has been well documented (e.g. Conte and De Boor, 1980).

For the system concerned, the initial estimation is more difficult than for the usual system of nonlinear equations since in each iteration the activity coefficients for all components have to be calculated. Making things even worse is that the analysis of brines from the field usually has some error, which causes the input inorganic ions not to be electroneutral. Physically, of course, this is incorrect. However, it is also difficult to justify which species should be adjusted. Therefore, in this model calculation is done from the direct input of analysis data if the departure from electroneutrality is less than 20%.

In this calculation, it was found that the Butler's (1964) initial scheme recommended by Zemaitis et al. (1986) was very difficult to apply and did not work well.

For the system, an initial estimation scheme was devised. The basic method is to calculate temperature dependent equilibrium constants and Henry's constants. From Henry's constant values the dissolved molecular species  $H_2S_L$  and  $H_2CO_3$  can be estimated. Then the pH value of the system is estimated. All the activity coefficients are set close to 1.0 except for  $S^{2-}$  and  $CO_3^{2-}$ , for which a value of 0.85 is set.

Given the above estimate, all other species can be estimated easily. In the program, this scheme is expressed in terms of an empirical correlation. Calculation experience showed that this scheme is very successful in converging.

### Solution of Mass Transfer Through Turbulent Layer

With all the parameter estimation given in the last chapter, equation (3.39) is integrated using the Runge-Kutta method. In each step, numerical integration of equation (3.43) is performed by Simpson's rule. Then,  $K^+$  is calculated through equation (3.47). Finally, equation (3.45) is used to obtain the mass transfer coefficients for the annular film flow.

### Solution of Diffusion Layer Model

The nonlinear equations (3.58) governing the system with the boundary conditions (3.60) and (3.61) are first linearized before being written in finite-difference form. Here the quasi-linearization method (Newman, 1973, Na, 1979) is used.

The basic idea for quasi-linearization is that one already has trial solutions and the change in these quantities during each iteration is relatively small. Then the nonlinear term in equation (3.58) can be written by assuming the trial solutions of  $C_i^\circ$  and  $\Phi^\circ$

$$C_1 \Phi'' = C_1^\circ \Phi'' + C_1^\circ (\Phi'' - \Phi^{\circ''}) + \Phi^{\circ''} (C_1 - C_1^\circ) + (C_1 - C_1^\circ) (\Phi'' - \Phi^{\circ''}) \quad (4.2)$$

Discarding the quadratic term and simplifying, one has

$$C_1 \Phi'' = C_1 \Phi^{\circ''} + C_1^\circ \Phi'' - C_1^\circ \Phi^{\circ''} \quad (4.3)$$

where the primes represent differentiation with respect to  $y$ . By treating the first derivative in an analogous manner, one has

$$C_1' \Phi' = C_1' \Phi^{\circ'} + C_1^{\circ'} \Phi' - C_1^{\circ'} \Phi^{\circ'} \quad (4.4)$$

Substitution of equations (4.3) and (4.4) into equation (3.58) gives the linearized equation as follows

$$\begin{aligned}
 D_i C_i'' + Z_i u_i F(C_i \Phi'' + C_i' \Phi'' + C_i' \Phi'' + C_i'' \Phi') \\
 = Z_i u_i F(C_i \Phi'' + C_i'' \Phi')
 \end{aligned} \tag{4.5}$$

Again by the similar treatment for the boundary condition equations (3.60) and (3.61), one has

For nonreactive species

$$D_i C_i' + Z_i u_i F(C_i \Phi'' + C_i' \Phi') = Z_i u_i F C_i' \Phi'' \tag{4.6}$$

For reactive species

$$D_i C_i' + Z_i u_i F(C_i \Phi'' + C_i' \Phi') = Z_i u_i F C_i' \Phi'' + I_i / nF \tag{4.7}$$

Linearized equations (4.5) with the boundary conditions (4.6), (4.7) and (3.63) can be solved by the finite difference method. The finite difference representation of the first and second derivatives are the central difference formulas

$$C_i'' = \frac{C_i(j+1) - 2C_i(j) + C_i(j-1)}{h^2} \tag{4.8}$$

$$C_i' = \frac{C_i(j+1) - C_i(j-1)}{2h} \tag{4.9}$$

$$\Phi'' = \frac{\Phi(j+1) - 2\Phi(j) + \Phi(j-1)}{h^2} \tag{4.10}$$

$$\Phi' = \frac{\Phi(j+1) - \Phi(j-1)}{2h} \quad (4.11)$$

The final finite difference form of equation (4.5) is

$$\begin{aligned} & C_i(j-1)(D_i - 1/2Z_i u_i Fh\Phi''') + C_i(j)(-2D_i + Z_i u_i Fh^2\Phi''') \\ & + C_i(j+1)(D_i + 1/2Z_i u_i Fh\Phi''') + \Phi(j-1)Z_i u_i F(C_i'' - 1/2hC_i''') \\ & + \Phi(j)(-2Z_i u_i FhC_i''') + \Phi(j+1)Z_i u_i F(C_i'' + 1/2hC_i''') \\ & = Z_i u_i Fh^2(C_i''\Phi'' + C_i'''\Phi''') \end{aligned} \quad (4.12)$$

The boundary condition can be expressed in a similar way.

$$\begin{aligned} & -D_i C_i(j-1) + C_i(j)2hZ_i u_i F\Phi'' + D_i C_i(j+1) \\ & -\Phi(j-1)Z_i u_i FC_i'' + \Phi(j+1)Z_i u_i FC_i'' \\ & = 2hZ_i u_i FC_i''\Phi'' + 2hI_i/nF \end{aligned} \quad (4.13)$$

In equation (4.13) for nonreactive species  $I_i$  equal to zero.

These system algebraic equations are solved by using the subroutine BAND(J) (Newman, 1973). The same solution procedure is also applied to solve the problem of mass transfer through the corrosion product layer.

#### Overall Computational Strategy

This model is built on the basis of previous work by Robertson (1988) under the guidance of Dr. Erbar, whose

work is based on GPA\*SIM developed by Erbar(1980). The calculation in this whole framework involves the phase equilibrium, pressure gradient, two phase flow regime and corrosion rate. The overall computational strategy is given in Figure 3.

Based on the strategy set up in GPA\*SIM, after some basic input, such as total gas flow rate, gas composition, well head temperature and pressure, bottom hole temperature and pressure, amount of water in the separator, and total depth of the well etc., the total depth of the well is divided into sections. Each section is assumed to be in uniform temperature and pressure upon which fluid phase equilibrium calculations are based. If the calculation results show that water has condensed or formation water is contained, the calculations of corrosion rate are performed as discussed above.

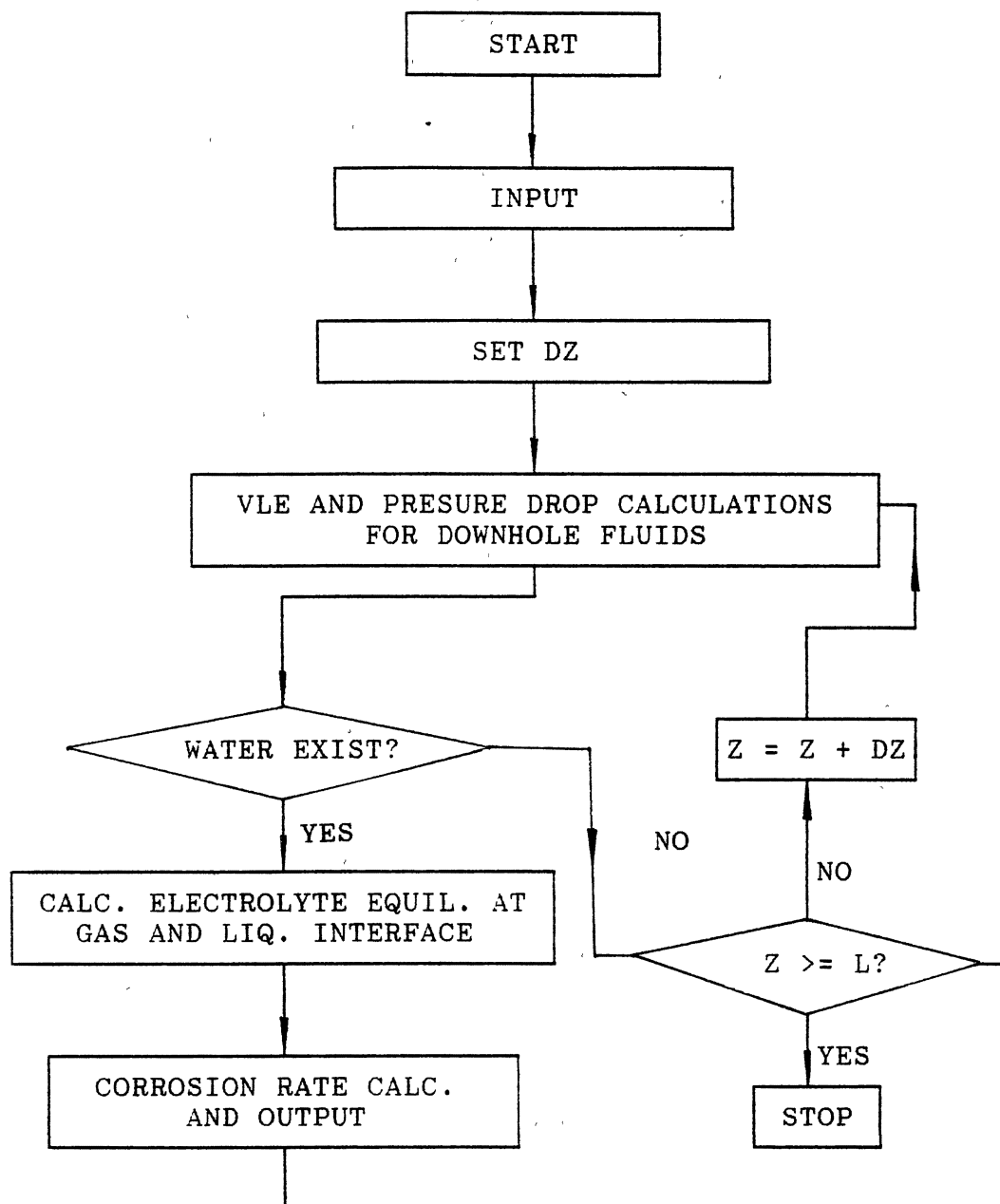


Figure 3. Flow Chart of Downhole Corrosion Program

## CHAPTER V

### RESULTS AND DISCUSSIONS

#### The Effect of CO<sub>2</sub> and H<sub>2</sub>S Partial Pressure

The purpose of this test of the influence of the partial pressure of CO<sub>2</sub> and H<sub>2</sub>S is to check the assumed cathodic and anodic reaction mechanisms. The direct comparison of the model results with experimental data is not very meaningful since most of the experimental data were taken from single phase liquid flow while the model is set up for annular gas-liquid two-phase flow. However, if under certain parameter combinations the model prediction can "match" the experimental data it can be used to check the assumed surface reaction mechanisms and mass transfer effect, which will be discussed later.

Figures 4 and 5 are typical calculation results of this model. Also in these Figures some experimental data and predictions by the De Waard and Milliams (1975) nomograph are given. All the model predictions are based on a pipe ID 2.467 inches and a pressure gradient of 14.4 lbf/ft<sup>3</sup>. Water flow rate is listed in the Figures.

From Figure 4 it is clear that the both De Waard and



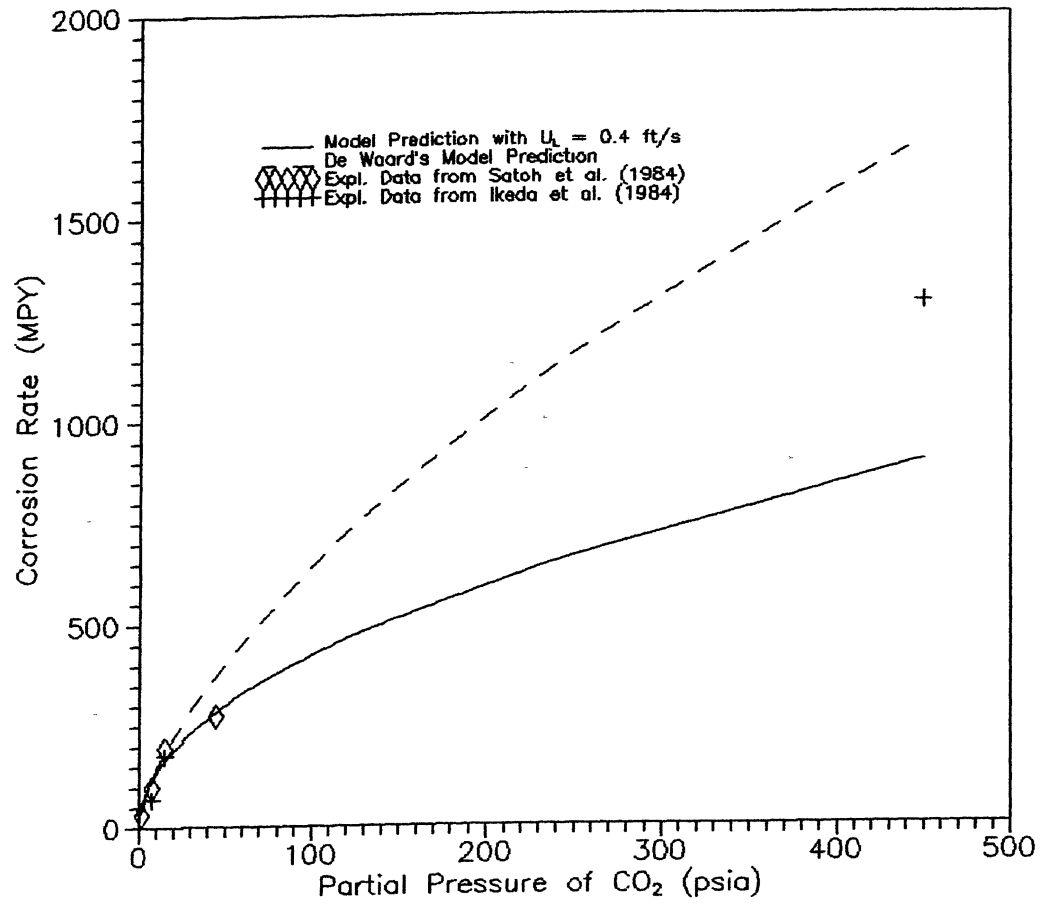


Figure 4. The Influence of CO<sub>2</sub> Partial Pressure on Corrosion Rate at 60 C Without Film

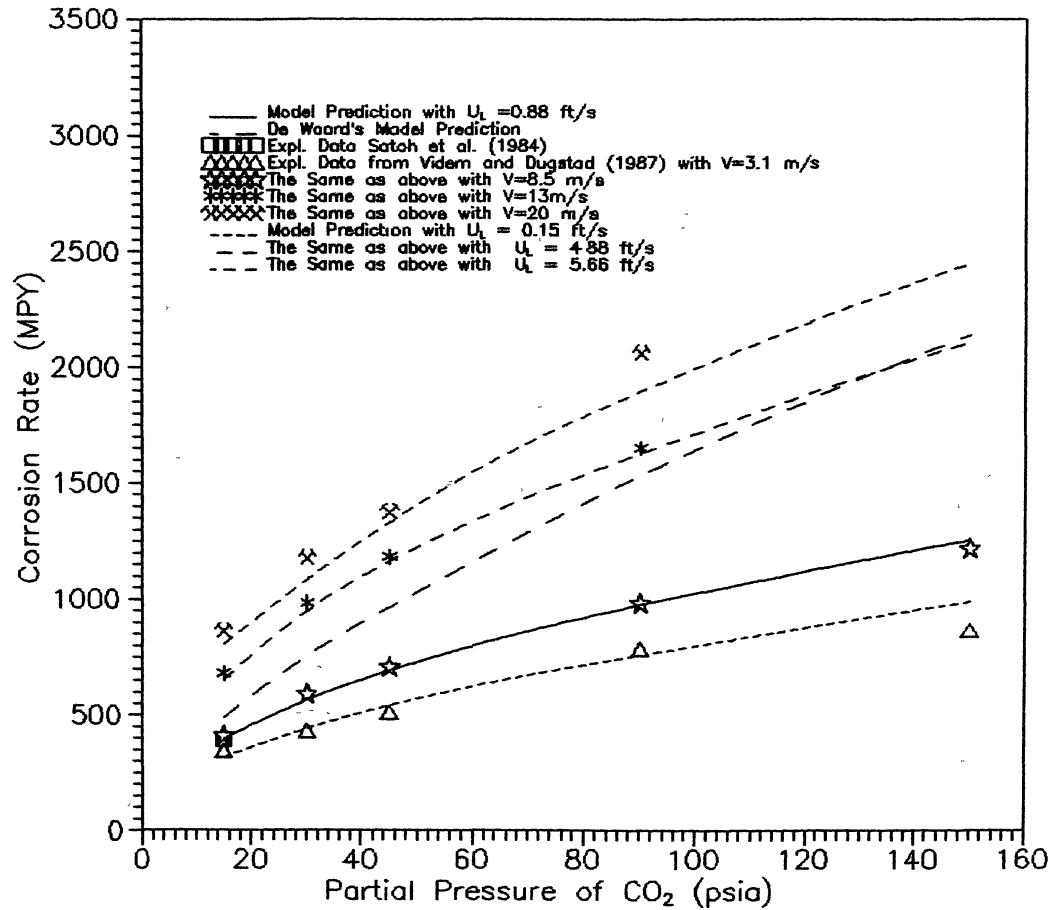


Figure 5. The Influence of CO<sub>2</sub> Partial Pressure on Corrosion Rate at 90 C Without Film

Milliams' model and this work give reasonable representation of experimental data when the partial pressure of CO<sub>2</sub> is below about 30 psi. However, the only high pressure data point falls in between the predictions of these two models. Under this constant liquid flow rate this model predicts lower corrosion rate while De Waard's model gives a higher value.

From Figure 5 it can be seen that this model can match the experimental data very well. In contrast, the model by De Waard and Milliams (1975) seems to give the wrong trend in the dependence of the partial pressure in the lower experimental flow rates. One may notice that this model has assumed the same surface reaction mechanisms as that of De Waard and Milliams, who have not given any exchange current density. However, the value of exchange current density will not change the dependence of the corrosion rate upon the partial pressure of CO<sub>2</sub>. Therefore, the only explanation is the mass transfer effect, which was found to be negligible in the range of their experiments.

A special note is worth giving about the model of De Waard and Milliams (1975). As has been mentioned in the literature survey, De Waard's model is based on a set of electrochemical experimental data which covers temperatures up to 80°C and partial pressures of CO<sub>2</sub> up to 15 psi. No mass transfer effect has been found when the liquid flow rate is above 3.3 ft/s. In fact, all later calculations of

corrosion rates are based on the correlation of their experimental data by Deberry and Yost (1984). As can be seen at higher partial pressures of CO<sub>2</sub> the mass transfer effect can not be neglected. A similar note about the De Waard and Milliams model has also been given by Schmitt (1984), who has pointed out that the De Waard and Milliams model can only apply to CO<sub>2</sub> partial pressures at less than 30 psia and temperatures up to 60°C.

Having said this, some of the phenomena can be explained reasonably. That this model can match the experimental data and De Waard's model in the low CO<sub>2</sub> partial pressure range probably means that the surface reaction mechanisms are reasonable. Since the mechanism used in this model implies that the reaction is first order for cathodic reactions and zero order for anodic reactions, the total corrosion rate depends approximately linearly upon the surface concentration of H<sub>2</sub>CO<sub>3</sub>. At low CO<sub>2</sub> partial pressures the concentrations of H<sub>2</sub>CO<sub>3</sub> are very low. Hence, the total corrosion rate is slow. Above a certain experimental fluid velocity no mass transfer effect is quite good as an approximation. However, when the partial pressure of CO<sub>2</sub> becomes higher, the situation changes as seen from Figure 5.

Figure 6 shows the influence of H<sub>2</sub>S partial pressure on the corrosion rate at 25°C. In this Figure, data from the correlation by Bartonicek (1969) are also shown. The

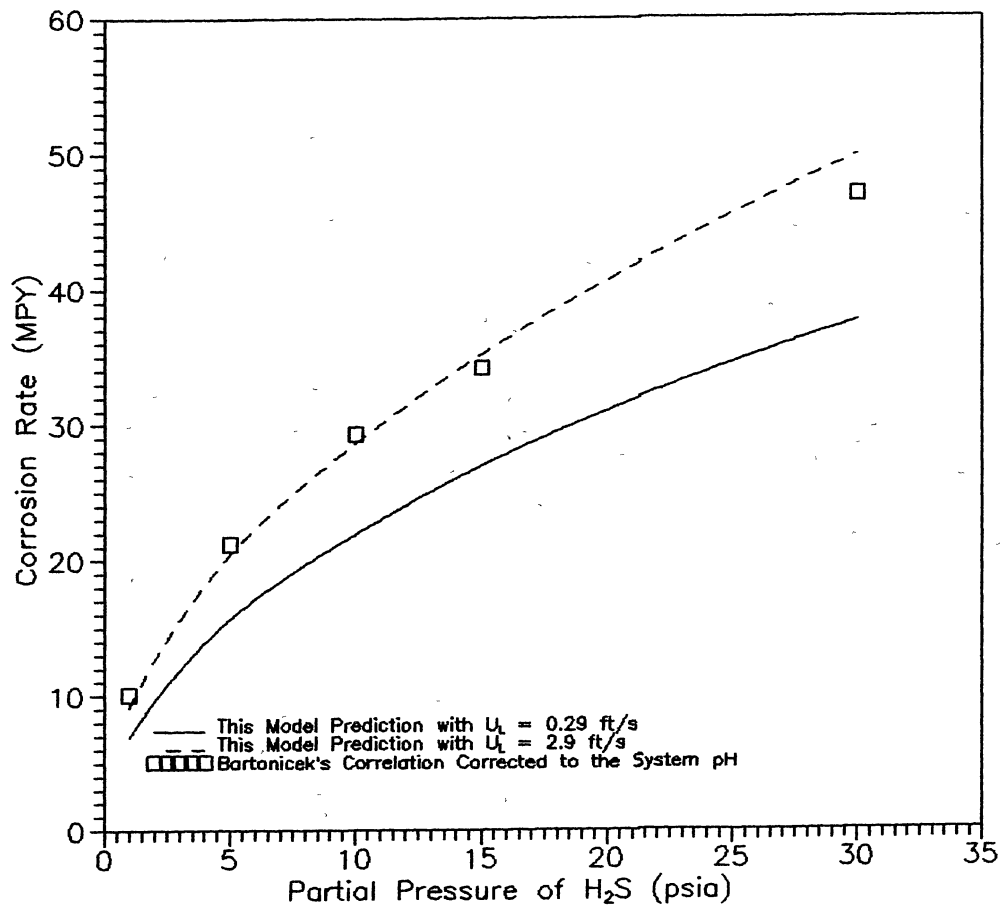


Figure 6. The Influence of H<sub>2</sub>S Partial Pressure on Corrosion Rate at 25 C Without Film

correlation by Bartonicek (1969) was expressed as

$$i_{\text{corr}} = i_0 p_{\text{H}_2\text{S}}^{0.2} \text{ (A/cm}^2\text{)} \quad (5.1)$$

where  $i_0 = 3.1 \times 10^{-4}$  at  $\text{pH} = 3$  and  $p_{\text{H}_2\text{S}}$  in atm. The data shown in Figure 6 was corrected by the relation that

$$d \log i_0 / d \text{pH} = - 0.5 \quad (5.2)$$

This relation was given by Bockris et al. (1961) and Morris et al. (1980).

It can be seen that the results of this model are quite comparable with Bartonicek's correlation. The dependence of the corrosion rate upon  $\text{H}_2\text{S}$  partial pressure from this model seems stronger than that from Bartonicek's correlation. One reason is that Bartonicek's correlation is only good up to 1 atm partial pressure of  $\text{H}_2\text{S}$ . Another is that the first order reaction with respect to  $\text{H}_2\text{S}$  in cathodic reaction assumed in the model should result in the stronger  $\text{H}_2\text{S}$  partial pressure dependence. However, the assumed mechanism seems quite reasonable if one considers that Bartonicek's correlation was developed at  $\text{pH} = 3$ , while  $\text{pH}$  for the system ranges from 4.0 to 4.8.

Figure 7 shows the corrosion rate at different  $\text{CO}_2$  partial pressures together with the experimental data from Greco and Wright (1962) and Rhodes and Clark (1936).



Again, it should be emphasized that the direct comparison between one phase flow experimental data and the results of two-phase flow calculations is not proper. In fact, both experimental data sets were taken in static solutions. Therefore, the agreement between this model and the experimental data in Figure 7. is, in one sense, coincidental. However, it can be seen that the trend of dependence of the corrosion rate on the CO<sub>2</sub> partial pressure is roughly the same between experimental data and this model, although under low liquid flow rate this model will predict the corrosion rate substantially lower. If one looks at the experimental conditions used by Greco and Wright (1962) and Rhodes and Clark (1936), one finds that the experiment only lasted two or three days. In this short period, no guarantee can be made that the surface is totally covered by the corrosion protective film. For example, Jasinski (1987) found that at CO<sub>2</sub> partial pressure 125 psi and room temperature the corrosion rate in the tap water can be as high as 120 mills per year (MPY) within 72 hours. This value definitely means that surface is not fully covered by corrosion film. On the other hand, Bradburn (1977) reported that under downhole conditions the corrosion rate may as low as 1 MPY at various temperatures and partial pressures of CO<sub>2</sub>.

From another sense, this agreement of the model results with experimental data shown in Figure 7 makes it



possible to explore some mechanisms showing why corrosion product has a protective effect on metals. Through computations it was found that the retardation of the corrosion rate in the presence of  $\text{FeCO}_3$  film is because of the shift of anodic equilibrium potential towards a more positive direction. For example, at  $25^\circ\text{C}$  and 15 psi partial pressure of  $\text{CO}_2$  the equilibrium potential is  $-0.618$  V and the corrosion potential  $-0.266$  V with respect to hydrogen reference electrode without corrosion product. This equilibrium potential is shifted to  $-0.399$  V with the corrosion potential to be  $-0.157$  V when  $\text{FeCO}_3$  film is formed on the surface. The anodic equilibrium potential with a product film is quite close to the passive potential value  $-0.4$  V reported by Ogundele and White (1986). Therefore, the presence of corrosion products is much like the passive wall. The shift of potential means slowing down the surface reaction rate (see equations 3.67 and 3.68). This does not mean that mass transfer has no influence on the corrosion rate in the presence of a corrosion product film since mass transfer would influence the concentrations of various ions on the surface. Therefore, the mass transfer rate here mainly contributes to the change of equilibrium potential. This point will be returned to later.

Figure 8 shows the influence of  $\text{H}_2\text{S}$  partial pressure on the corrosion rate with a protective film. Since only

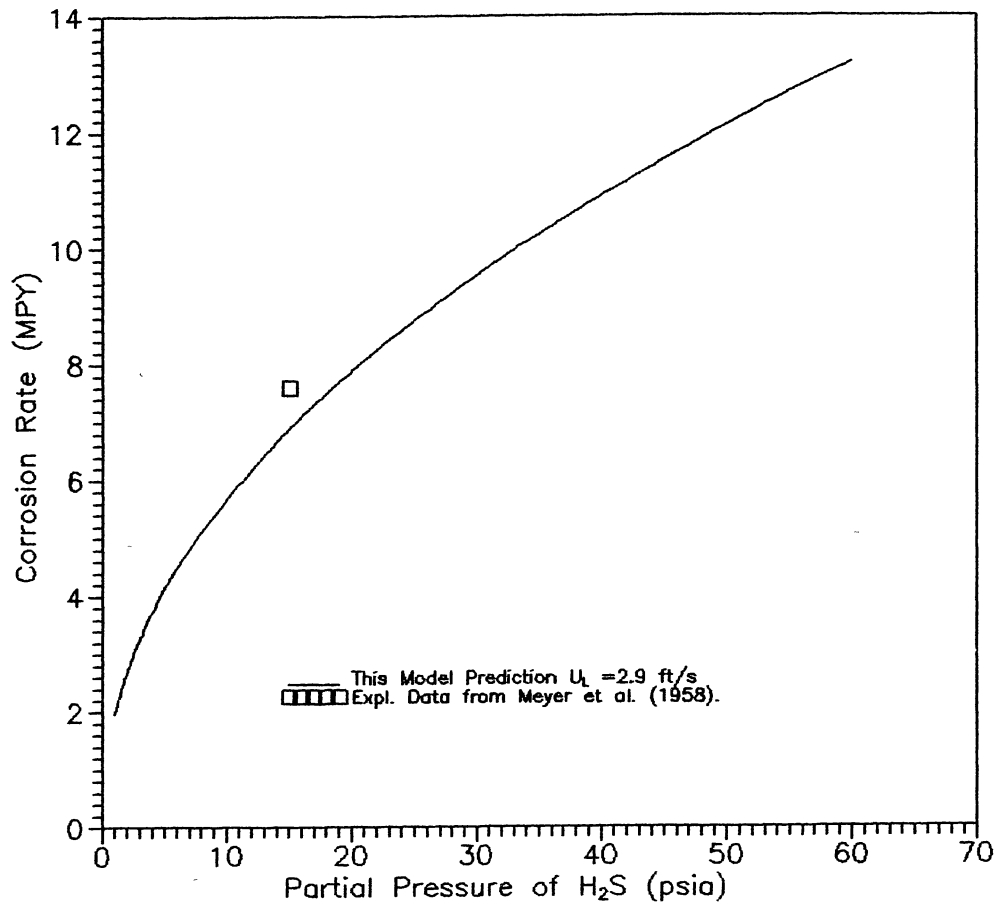


Figure 8. The Influence of H<sub>2</sub>S Partial Pressure on Corrosion Rate at 25 C with Film

experimental data from Meyer et al. (1958) has been found not much can be said for the comparison. The decrease in the corrosion rate in the presence of FeS is by the same mechanism as in the CO<sub>2</sub> corrosion system, i.e. the formation of a corrosion product film decreases the driving potential between  $E_{corr}$  and equilibrium potential.

#### The Effect of Flow Rate

Both gas and liquid flow rates have influence on the corrosion rate. However, the impact of gas flow rate on the corrosion rate is through its increase in the interfacial stress. In the model, the input pressure gradient is used in the calculation wall shear stress since this treatment will minimize the error for mass transfer caused by inaccuracy of downhole pressure gradient calculations. Therefore, the discussion of influence of gas flow rate on the corrosion rate will be delayed until the section of real downhole corrosion simulations. In this section, only the effect of liquid flow rate will be addressed.

Figure 9 is a comparison of this model prediction with the experimental data from Eriksrud and Søntvedt (1984), who have studied the corrosion of carbon steel under slug flow. This model prediction is under the same conditions as the experiments. As shown in Figure 9 the agreement between the model prediction and experimental data is quite

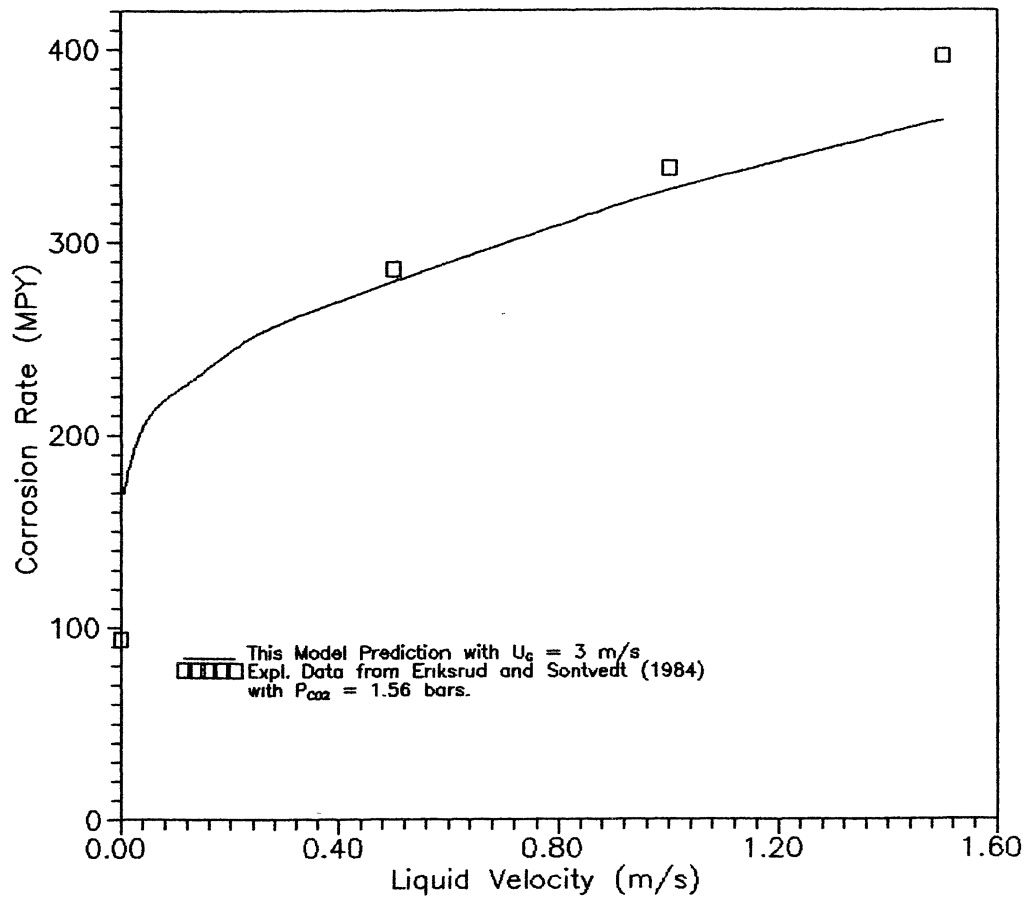


Figure 9. The Influence of Liquid Flow Rate on Corrosion Rate at 60 C in 4% NaCl Without Film

good. At a liquid flow rate of 1.5 m/s, this model predicts about 10% lower than the experimental data. This seems to confirm that uniform corrosion under slug flow can be treated as if it were in annular flow (see assumption (5) in chapter III) and the increase in the corrosion rate by slug flow is much more localized corrosion related. Furthermore, this also indirectly justifies the mass transfer model developed in this work. It should be pointed out that only one set of experimental data is not sufficient to validate the model completely. More experimental data are needed to understand the corrosion processes in two-phase flow.

Figure 10 shows the influence of mass transfer on the corrosion rate with a corrosion product film. No data are available for comparison of the model prediction. Comparing Figure 10 with Figure 9 one can see that the enhancement in the corrosion rate by mass transfer is weaker in the presence of film than without corrosion product. In fact, in the range of liquid flow rates compared the corrosion rate increases by a factor of 1.7 without a protective film and of 1.3 with the film. As has been mentioned in the previous section, the retardation effect of the corrosion product film is mainly to shift the equilibrium potential towards a more positive value. This process is very similar to passivation, in which flow contributes to passivation by shifting the corrosion

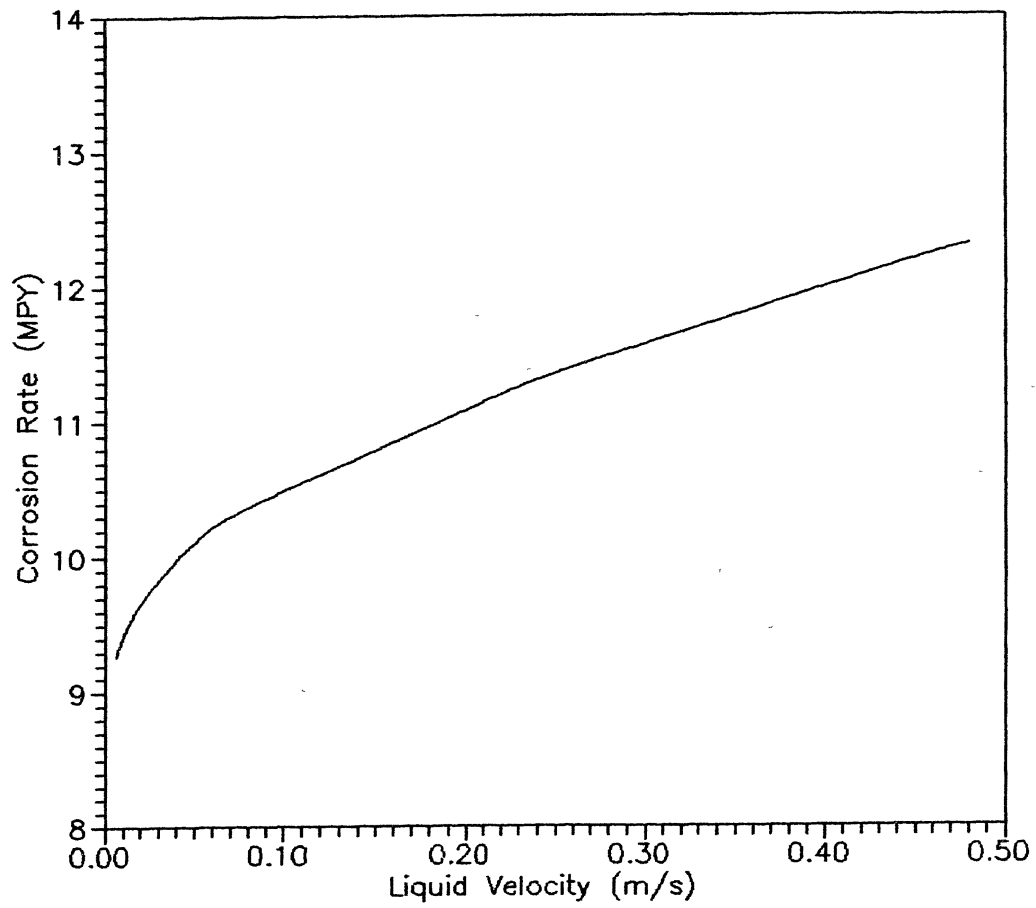


Figure 10. The Influence of Liquid Flow Rate on Corrosion Rate at 60 C in 4% NaCl with Film

potential.

### Some Downhole Cases

In this section, the model prediction will be compared with some field data. It should be noted this model development is based on the assumption of uniform corrosion. This rarely happens downhole. Most of the downhole corrosion processes are localized in nature. Therefore, in this sense direct comparison is not possible. However, as has been pointed out the model will serve as a departure for the further study of downhole corrosion. For another, this model calculates the uniform corrosion rate with or without a corrosion product film. Uniform corrosion without a solid protective film is the worst situation on one hand. On the other hand, uniform corrosion with a protective film should represent the "best" scenario. Therefore, this model should bound the corrosion process downhole and give a practical guide to the prediction of the corrosion rate to the corrosion engineer.

#### Case I

Case I is a corrosive well. After four years of service the pipe in the well has many places that have holes owing to corrosion. The gas well conditions for this case are given in Table IV, V and VI. The model results

together with the field data are presented in Figure 11.

From Figure 11 it can be seen that this model seems to serve our purposes pretty well for this case. The

TABLE IV  
GAS COMPOSITION OF THE WELL  
FOR CASE I

Component	Mol Percent
Methane	90.94
Ethane	4.37
Propane	1.14
I-butane	0.27
N-butane	0.23
I-pentane	0.13
N-pentane	0.08
Hexanes	0.11
Heptanes Plus	0.27
Nitrogen	0.25
Carbon Dioxide	2.21
Totals	100.00



TABLE V  
WATER ANALYSIS OF GAS WELL  
FOR CASE I

Constituents	PPM
Sodium	6490
Calcium	298
Magnesium	38
Barium	4
Iron	36
Chloride	10100
Sulfate	111
Bicarbonate	879
Total Dissolved Solids	17956

TABLE VI  
WELL CONDITIONS FOR CASE I

Specifications	Units	Value
Water Production	B/D	28
Gas Production	MSCFD	2150
Depth	ft	9700
Tubing Diameter, ID	in.	2.441
Wellhead Pressure	psia	1890
Wellhead Temperature	°F	130
Bottomhole Pressure	psia	4000
Bottomhole Temperature	°F	290

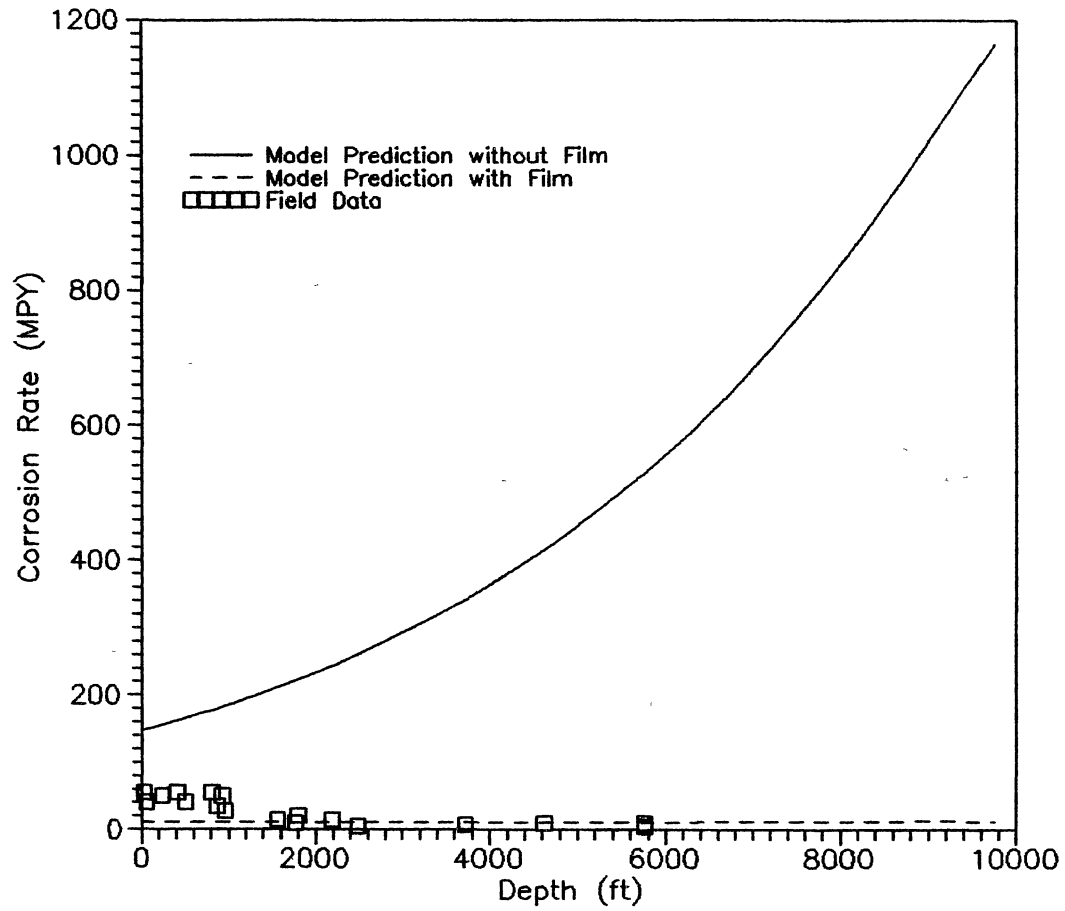


Figure 11. The Corrosion Rate Profile Along Depth for Case I

corrosion rate without a protective film is very high compared with the field data. Furthermore, the temperature and pressure dependence is also much stronger than that of the field data. There is no surprise about this since downhole corrosion occurs with a protective film. The corrosion rate with a protective film predicted from the model bounded most of the observed data. However, this model does have some deficiency in terms of the position of the corrosion starting point. As shown in Figure 11 this model predicts that the corrosion starts from the very bottom of the hole. In contrast, the observed corrosion position begins at a depth of about 6000 ft. This inconsistency may result from two possible reasons. The position of water condensation, which is assumed to be a necessary condition for corrosion to occur, predicted from the thermodynamic calculation may have some error for one reason. For another, the model in the prediction of the corrosion rate with a protective film may need further work since some laboratory data (Ikeda et al., 1984, Hausler, 1984) have showed that the protective film is more effective when the temperature is above 120°C. However, at this stage we do not have enough quantitative information to characterize the  $\text{FeCO}_3$  film at different temperatures. With more information accumulated this part of the model can be modified easily. However, it should be noticed that downhole corrosion is a complex system for which there are

many exceptions unknown to us. This point will be picked up in the discussion of Case III.

The possible cause for this well to be relatively corrosive (in four years of production there are many holes or parting of the pipe) is its relative high concentration of CO<sub>2</sub> in the gas phase (see Table IV) because it can be seen from Table IV this well has moderate water production rate and not very high gas production rate. The brine produced may not be the reason for the higher corrosion rate. This point will be returned to later.

#### Case II

Case II is a noncorrosive well. The well conditions are listed in Table VII, VIII and IX. The model results are given in Figure 12. The field measurement showed that the corrosion rate is less than 7.5 MPY, which is not distinguishable for the measurement. This model predicts a corrosion rate of 4.0 MPY with a protective film on the wall. This is quite comparable to the field observations. Therefore, it seems that the model can also predict the behavior of noncorrosive wells. As has been pointed out by Crolet and Bonis (1984), the prediction of noncorrosiveness for a well is equally important. The main reason for the small corrosion rate of this well is its lower CO<sub>2</sub> content in the gas phase.

It can be seen that the well in Case II has higher

water and gas production rates compared with Case I but the corrosion rate is much lower for case II than for Case I. Therefore, for these two cases the production rates of the gas and water is not the dominant factor.

TABLE VII  
GAS COMPOSITION OF THE WELL  
FOR CASE II

Component	Mol Percent
Methane	90.10
Ethane	6.00
Propane	1.68
I-butane	0.45
N-butane	0.34
I-pentane	0.20
N-pentane	0.12
Hexanes	0.18
Heptanes Plus	0.40
Nitrogen	0.22
Carbon Dioxide	0.31
Totals	100.00

TABLE VIII  
WATER ANALYSIS OF GAS WELL  
FOR CASE II

Constituents	PPM
Sodium	127
Calcium	21
Magnesium	0
Barium	3
Iron	0
Chloride	195
Sulfate	0
Bicarbonate	60
Total Dissolved Solids	406

TABLE IX  
WELL CONDITIONS FOR CASE II

Specifications	Units	Value
Water Production	B/D	124
Gas Production	MSCFD	2800
Depth	ft	9620
Tubing Diameter, ID	in.	2.441
Wellhead Pressure	psia	1270
Wellhead Temperature	°F	130
Bottomhole Pressure	psia	4000
Bottomhole Temperature	°F	290



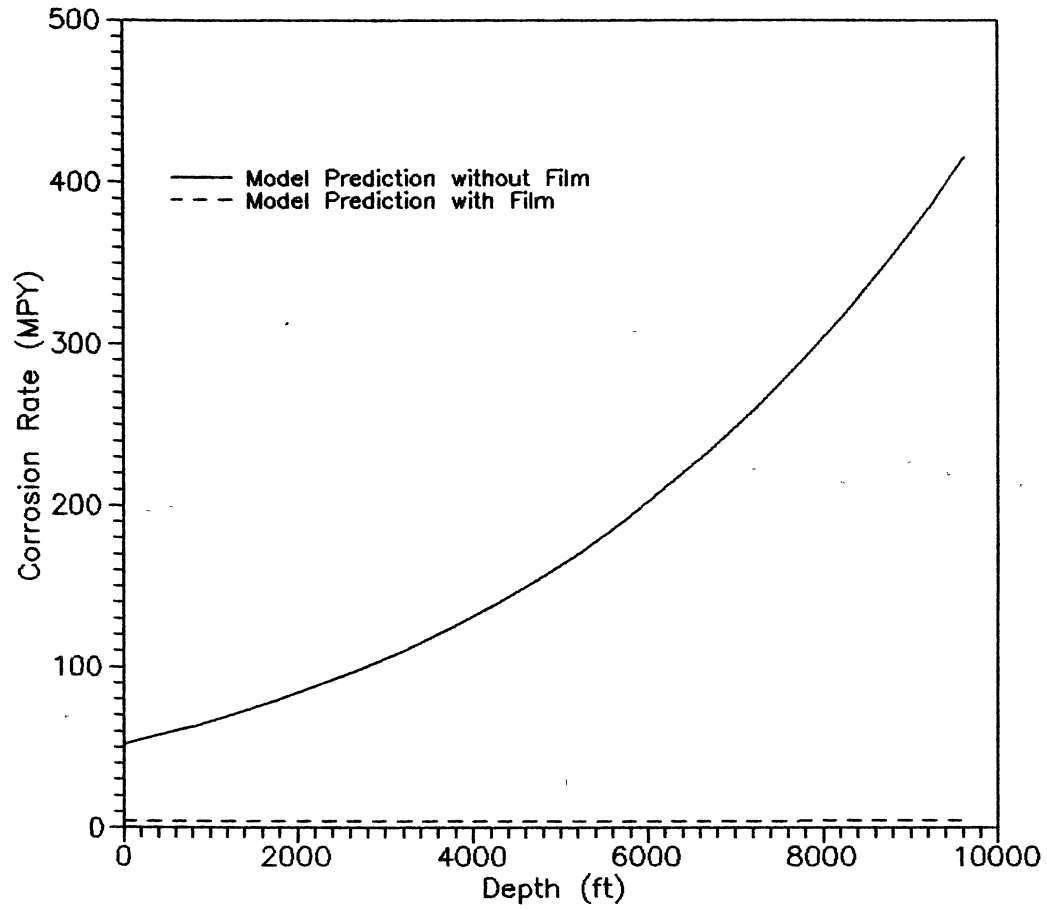


Figure 12. The Corrosion Rate Profile Along Depth for Case II

### Case III

Case III is a well with a moderate corrosion rate. The well conditions are presented in Table X, XI, and XII. The model results are given in Figure 13. Again, as in Case I, the predicted corrosion rate without a corrosion film is much higher than that of the field data. The corrosion rate with a protective film predicted from this model bounded most of the field data. It is impossible to bound all the field data because the observed field data include much localized corrosion. For localized corrosion, the corroded parts have a protective effect on those uncorroded parts.

Figure 14 is an enlargement of the corrosion rate with a protective film. For the sake of comparison, Figure 15 represents the corrosion rate with a protective film for Case I. From this two Figures, one can see that the model predicts the corrosiveness of these wells quite well. The field observed maximum corrosion rate for Case III is about 40% that of Case I. In contrast, this model predicts that the corrosion rate of Case II is about 46-60% that of Case I. From further comparison of the well conditions of these two cases, one would notice that these two wells produce almost the same brines. Therefore, as mentioned previously the brine compositions are not the dominant factor. For these two wells, the gas production rates and CO<sub>2</sub>

TABLE X  
GAS COMPOSITION OF THE WELL  
FOR CASE III

Component	Mol Percent
Methane	91.60
Ethane	4.39
Propane	1.18
I-butane	0.33
N-butane	0.25
I-pentane	0.14
N-pentane	0.09
Hexanes	0.13
Heptanes Plus	0.33
Nitrogen	0.30
Carbon Dioxide	1.26
Totals	100.00

TABLE XI  
WATER ANALYSIS OF GAS WELL  
FOR CASE III

Constituents	PPM
Sodium	6280
Calcium	454
Magnesium	50
Barium	2
Iron	0
Chloride	10300
Sulfate	196
Bicarbonate	313
Total Dissolved Solids	17595

TABLE XII  
WELL CONDITIONS FOR CASE III

Specifications	Units	Value
Water Production	B/D	27
Gas Production	MSCFD	1352
Depth	ft	9450
Tubing Diameter, ID	in.	2.441
Wellhead Pressure	psia	1440
Wellhead Temperature	°F	130
Bottomhole Pressure	psia	4000
Bottomhole Temperature	°F	290

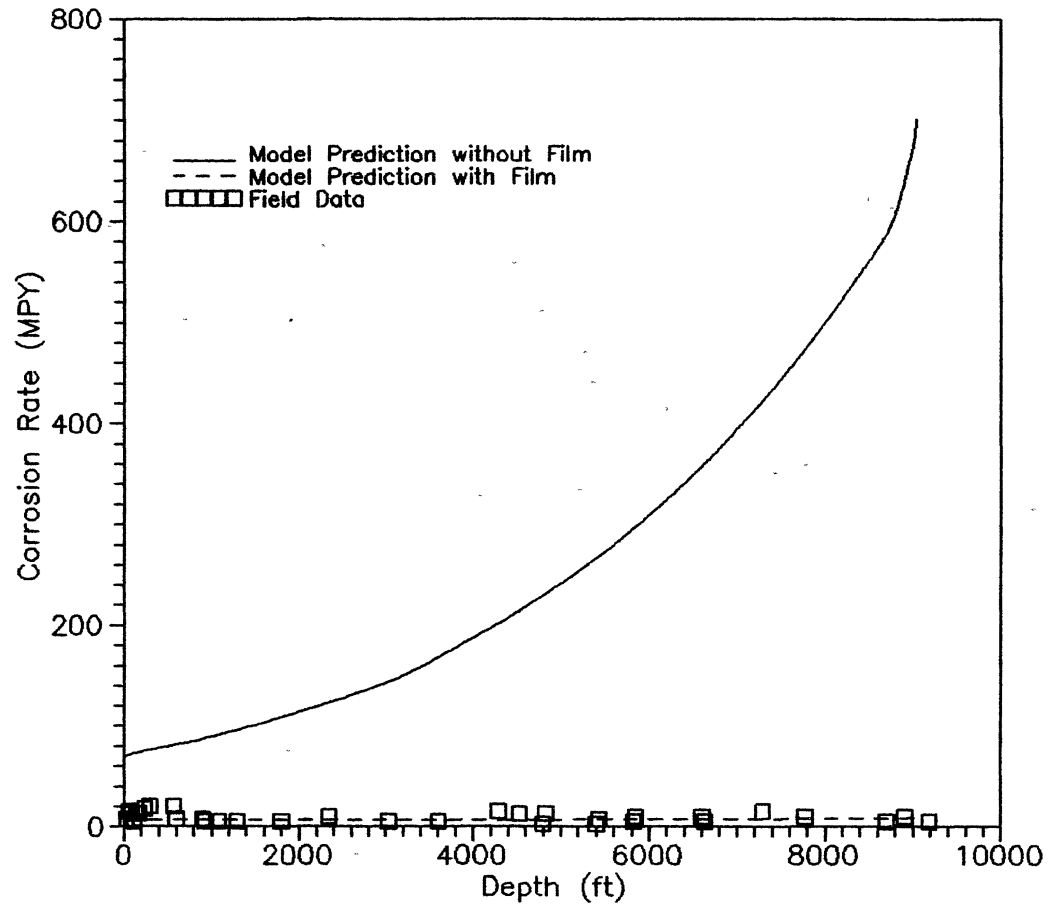


Figure 13. The Corrosion Rate Profile Along Depth for Case III

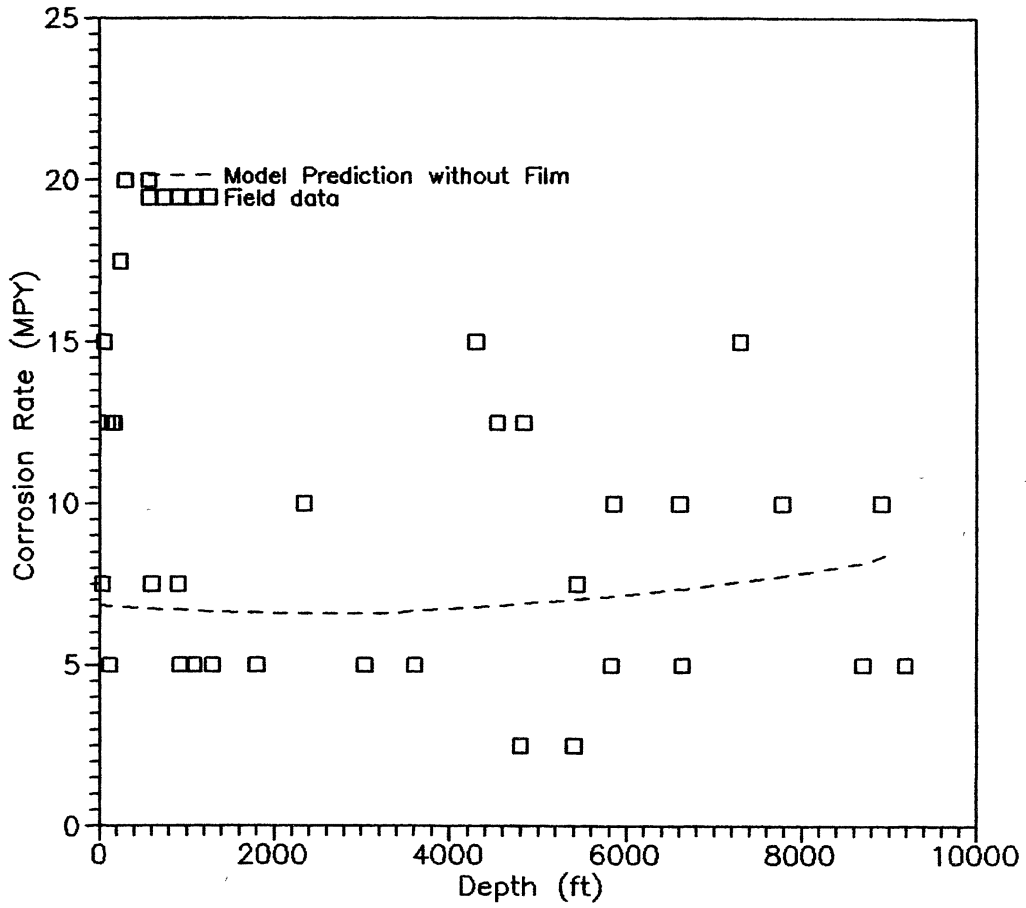


Figure 14. The Corrosion Rate Profile Along Depth for Case III with protective film

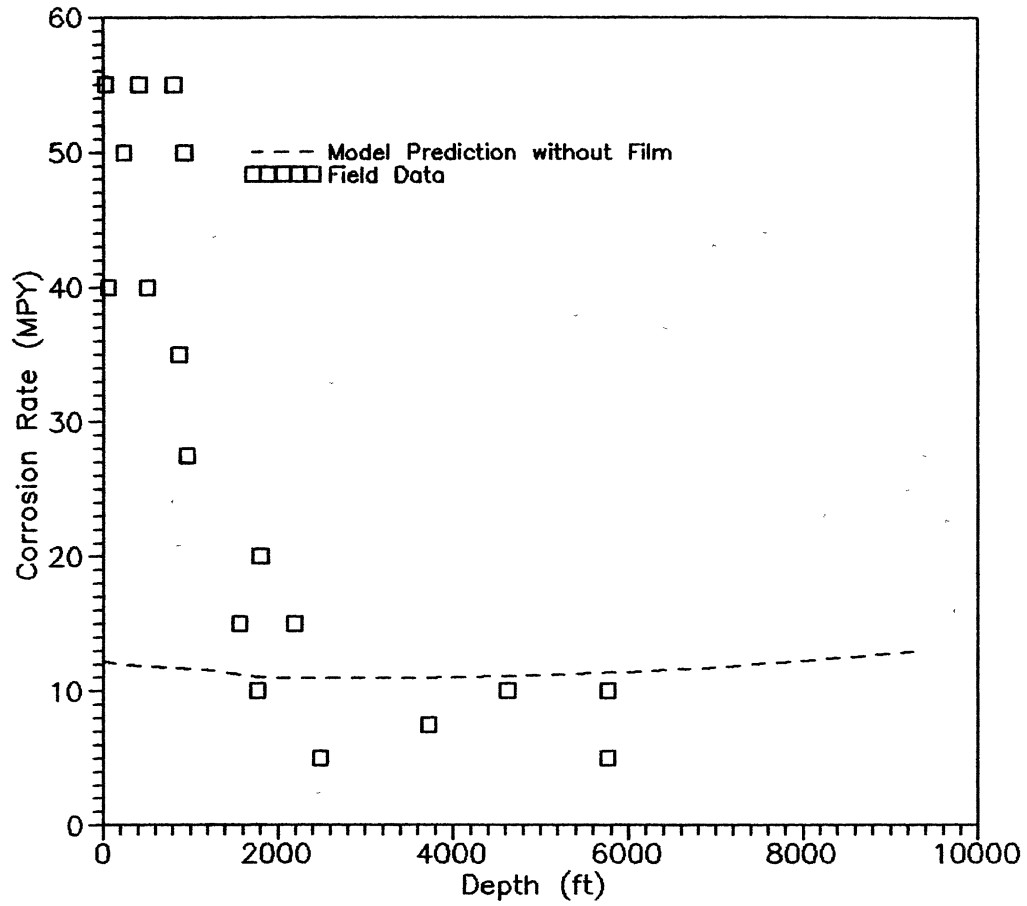


Figure 15. The Corrosion Rate Profile along Depth for Case I with Protective Film



composition are main factors to make the corrosion rate different. In the discussion for Case II, we have compared Case I with Case II and concluded that for the two cases the flow rate is not the dominant factor. Therefore, for a downhole corrosion system, trying to use a single index to predict the corrosion rate has little chance of success.

A further note on the comparison of Figure 14 and 15 is the starting position of corrosion. For both Cases I and III, the model predicts that corrosion will start right from bottom hole. However, as mentioned in the discussion of Case I, in that case corrosion starts from 6000 ft or above. For Case III, the field data indicates that the corrosion starts from the very bottom of the hole as predicted by the model. The observed difference of the starting corrosion depth for these two cases seems to have no simple explanation.

#### Case IV

Case IV is a well as corrosive as Case I. The well conditions for Case IV are presented in Tables XIII and XIV. A comparison of the well conditions of Case I and IV indicates that Case IV has a relatively high gas production rate. If one considers that the diameter of the pipe is smaller for Case IV than for Case I, the gas velocity in the well is much higher.

For this well, no water production was reported.

TABLE XIII  
GAS COMPOSITION OF THE WELL  
FOR CASE IV

Component	Mol Percent
Methane	90.44
Ethane	5.07
Propane	1.36
I-butane	0.32
N-butane	0.27
I-pentane	0.15
N-pentane	0.09
Hexanes	0.14
Heptanes Plus	0.32
Nitrogen	0.12
Carbon Dioxide	1.72
Totals	100.00

TABLE XIV  
WELL CONDITIONS FOR CASE IV

Specifications	Units	Value
Water Production	B/D	2.5
Gas Production	MSCFD	3320
Depth	ft	9540
Tubing Diameter, ID	in.	1.992
Wellhead Pressure	psia	2225
Wellhead Temperature	°F	130
Bottomhole Pressure	psia	4000
Bottomhole Temperature	°F	290

Therefore, no water analysis is available. In order to be able to apply the model, a water production rate of 2.5 barrels/day was assumed since, in general, if there were no water production from the well, there would have been no corrosion. Further, it was assumed that water does not contain any other inorganic ions except the disassociative ions from  $\text{CO}_2$  and  $\text{H}_2\text{O}$ .

Figure 16 shows the model prediction of the corrosion rate with a protective film together with the field data. It can be seen that this well is as corrosive as Case I and this model predicts the same corrosion rate as in Case I (see Figure 15). From the results, it seems that the model can distinguish the corrosive wells from those noncorrosive ones.

#### Case V

Case V is a gas well that was initially thought to be a "noncorrosive" one. After about 3 months operation, the well failed due to corrosion problems. The well conditions are given in Table XV, XVI and XVII. The gas composition for this well is not reported. The only known data is that there is 0.8% of  $\text{CO}_2$  in the gas analysis. The data listed in Table XV is an assumed composition for test of the model. Under normal circumstances, the corrosion behavior of a steel is not influenced by the presence of the hydrocarbon gases (Ogundele and White, 1987). Therefore,

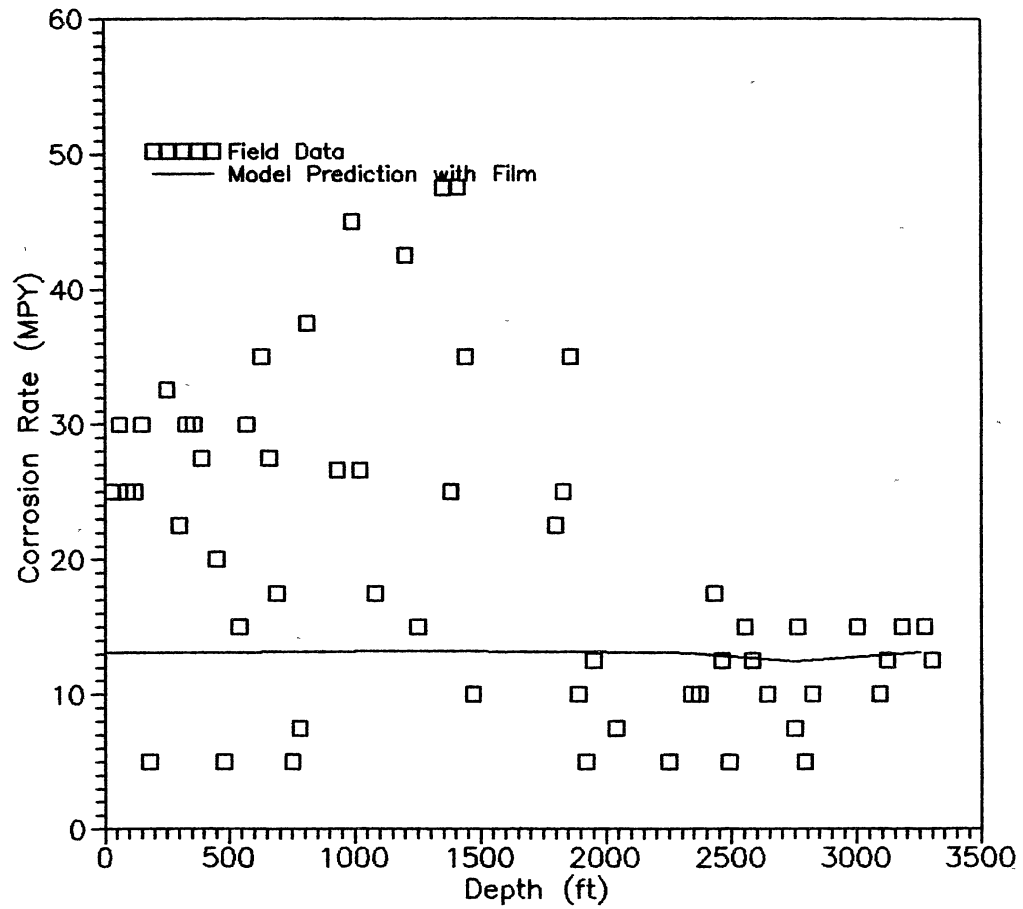


Figure 16. The Corrosion Rate Profile along Depth for Case IV with Protective Film

TABLE XV  
ASSUMED GAS COMPOSITION  
FOR CASE V

Component	Mol Percent
Methane	91.84
Ethane	4.59
Propane	1.36
I-butane	0.32
N-butane	0.27
I-pentane	0.15
N-pentane	0.09
Hexanes	0.14
Heptanes Plus	0.32
Nitrogen	0.12
Carbon Dioxide	0.80
Totals	100.00

TABLE XVI  
WATER ANALYSIS OF GAS WELL  
FOR CASE V

Constituents	PPM
Sodium	45121
Calcium	8880
Magnesium	864
Barium	17
Iron	31.5
Chloride	87500
Sulfate	248
Bicarbonate	205
Total Dissolved Solids	143834

TABLE XVII  
WELL CONDITIONS FOR CASE V

Specifications	Units	Value
Water Production	B/D	3500
Gas Production	MSCFD	5000
Depth	ft	13000
Tubing Diameter, ID	in.	2.441
Wellhead Pressure	psia	6400
Wellhead Temperature	°F	160
Bottomhole Pressure	psia	9300
Bottomhole Temperature	°F	290



assuming the hydrocarbon gas compositions is immaterial (except for the pressure, temperature and phase predictions).

Figure 17 shows the corrosion rate profiles along the depth of the well without a protective film. For the sake of comparison the predicted corrosion rates from the De Waard and Milliams' nomograph were also showed in Figure 17. The correlation from De Waard and Milliams predicts higher corrosion rates for this well owing to two reasons. One, already discussed, is that this correlation only applies up to 2 bars of CO<sub>2</sub> partial pressure. The other is this correlation only applies to systems with temperatures below 80°C. Above these temperature and partial pressure limits the correlation gives much higher corrosion rates. From Figure 17 it can be seen that the corrosion rates without a protective film from this model vary from 400 to 3000 MPY. The well failed in about 3 months, which means that the corrosion rate is on the order of 1000 MPY (the wall thickness 217 mils). Therefore, this case illustrates that the prediction of corrosion rate without a protective film is not totally impractical. However, it should be emphasized again that the same order of magnitude of the corrosion rate does not necessarily mean that the downhole corrosion processes are due to the same mechanisms as the model assumed. The speculation is that the high corrosion

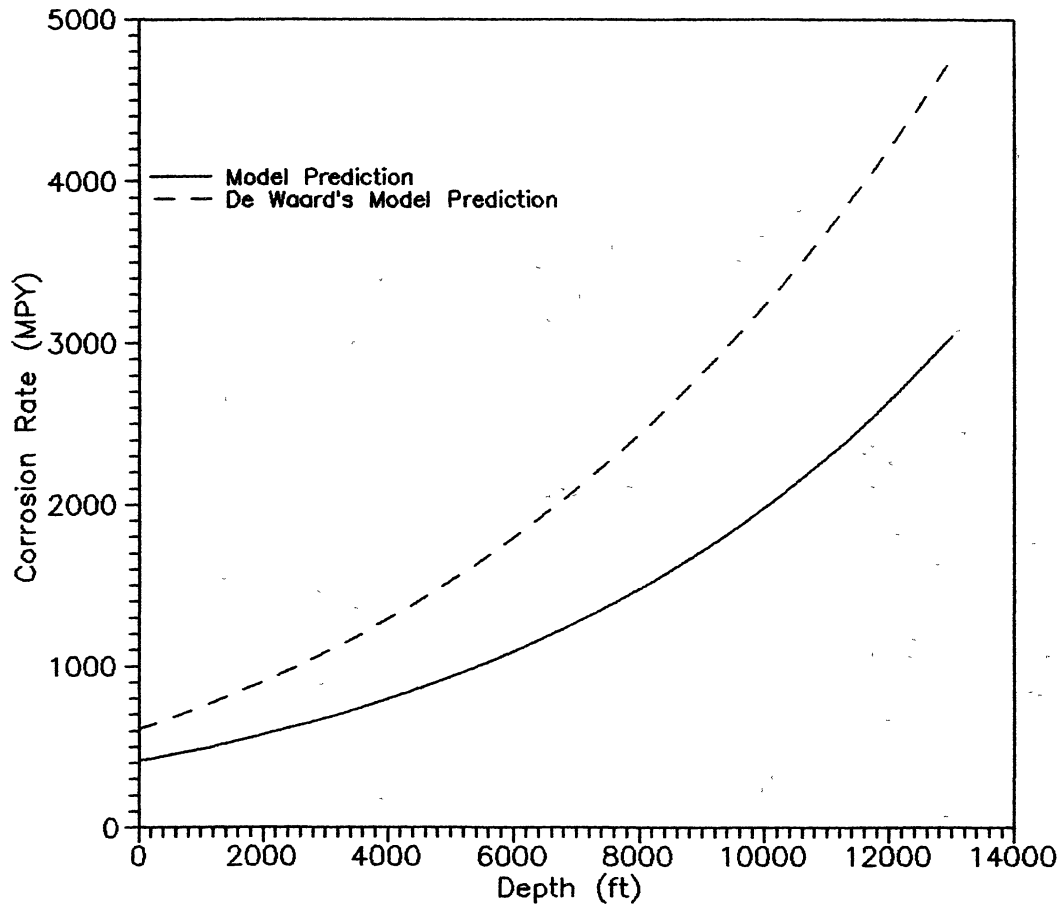


Figure 17. The Corrosion Rate Profile Along Depth for Case V Without Protective Film

rate of this well is due to slug flow, high solid content in the water and exceptionally high water production rate. Although calculated homogeneous fluid velocity is only 50% of the erosional velocity slug flow may cause a fatigue problem in the film. Therefore, the higher corrosion rate results.

Figure 18 shows the predicted corrosion rate with a protective film. Comparing Figure 18 with Figure 15 and 16, one can figure out that the corrosion rate for this well is about 50-70% higher than that of Cases I and IV. It means that the fluid in this well is definitely more corrosive than those in Cases I and IV, which had a real life-time of about four years. From this comparison, it shows again this model can distinguish the corrosive wells from the noncorrosive ones.

In summary, from the limited cases tested, we can tentatively set some interconnections between the model and the observed field data.

Corrosion without a protective film rarely occurs in gas wells. In other words, the predicted corrosion rate without a protective film is much higher than the real observed corrosion rate except for some special cases.

The predicted corrosion rate from the model with a protective film is lower than that of the maximum field observation. If the model predicts the corrosion rate to be less than 4 MPY, the well is generally noncorrosive. If

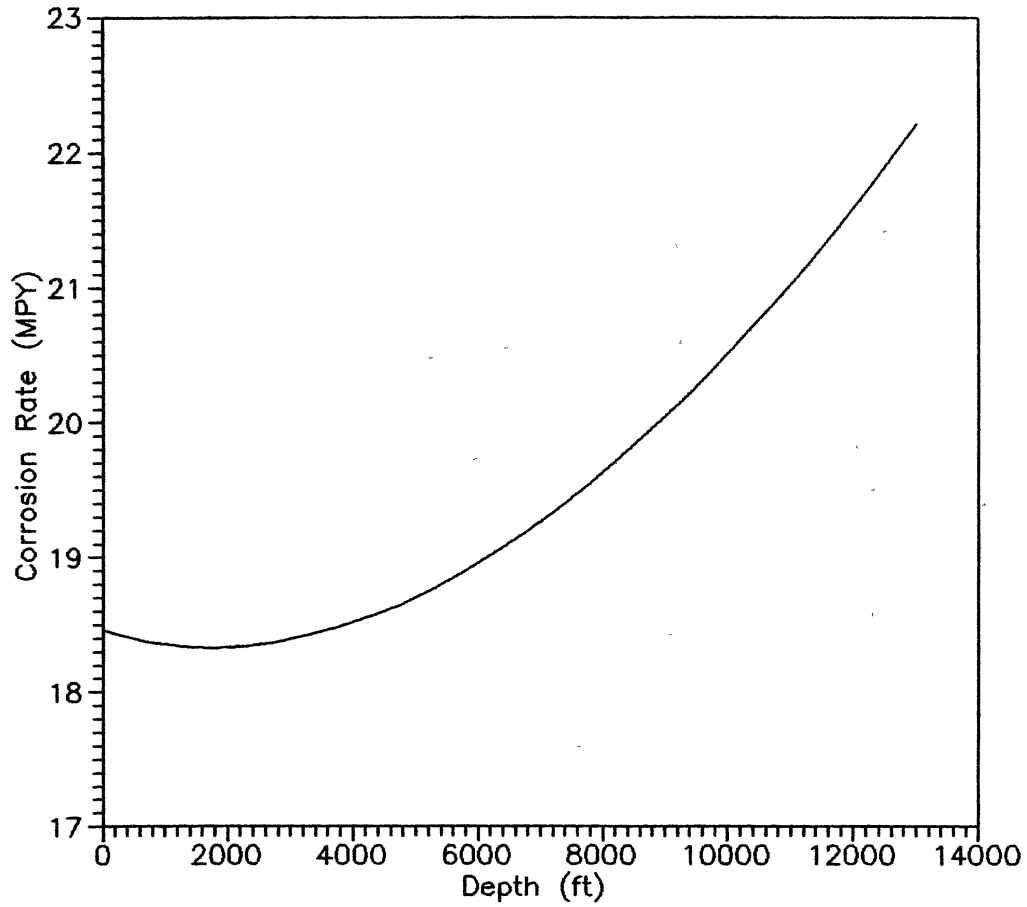


Figure 18. The Corrosion Rate Profile Along Depth for Case V with Protective Film

the model predicts the corrosion rate more than 12 MPY, the well should be corrosive. Those wells that have predicted corrosion rates between 4 and 12 MPY may be corrosive but probably the corrosion is not very severe.

## CHAPTER VI

### CONCLUSIONS AND RECOMMENDATIONS

#### Conclusions

1). A mathematical model has been developed for gas wells with annular two-phase gas-liquid flow. The model includes the calculations of the equilibrium concentration of various species, the mass transfer process through a strongly gas sheared turbulent liquid film and a diffusion layer, and the surface electrochemical reactions. Generally speaking, the model represents experimental data well.

2). For the uniform corrosion rate without a corrosion product film, the corrosion mechanism for both  $\text{CO}_2$  and  $\text{H}_2\text{S}$  containing brines can be described as a first order reaction of molecules of  $\text{H}_2\text{S}$  and  $\text{H}_2\text{CO}_3$ .

3). The widely used De Waard and Milliams nomograph can only be applied to the systems that have a  $\text{CO}_2$  partial pressure less than 2 bars. At higher partial pressures, this nomograph will give much higher corrosion rates.

4). Most experimental and field data show that mass transfer effects are very strong. For a two-phase flow system increasing both gas and liquid flow rate will

increase corrosion rate substantially. In contrast, the assumption of no mass transfer effects in De Waard and Millims's nomograph is in error.

5). Compared with limited field data, the corrosion rates without a protective film predicted from this model are much higher. This means that the corrosion processes downhole in gas wells occurred with a protective film.

6). The corrosion rates with the protective films predicted from this model are much nearer the field data, although lower than maximum observed corrosion rates. The direct comparison of the model prediction with field data seems impossible because downhole corrosion is very localized in nature. The tentative criteria were set up for practical applications of the prediction of the corrosiveness of a gas well through a limited test of the model. If the predicted corrosion rate with a solid film is less than 4 MPY, the well is noncorrosive. If the predicted corrosion rate is greater than 12 MPY, the well is corrosive. At any value between them, the well probably is moderately corrosive, but not very severely so.

7). Many factors have some influence on the corrosion rate. The preeminent parameters are gas and liquid flow rates and CO<sub>2</sub> partial pressures, depending upon the system conditions. Trying to use any single variable as an index to predict downhole corrosion is not a very promising approach.

## Recommendations

### Modeling Localized Corrosion

Localized corrosion, in practice, is more important than uniform corrosion and it is more difficult to simulate. The so-called localized corrosion includes all the forms of corrosion with the appearance that some parts of the metal are more severely corroded than other parts. The cause of this type of corrosion, the author believes, is rarely by the usual sense of pitting corrosion for downhole. Taking the downhole corrosion under slug flow with CO<sub>2</sub> and H<sub>2</sub>S containing brines as an example, one can imagine the picture of the process as follows: After an initial fast corrosion rate a protective corrosion product film will be formed on the metal wall. When the fluid flowing in the pipe is in slug flow, a section of pipe will "feel" periodic up and down liquid flow and actions of gas bubbles. When the bullet type of Taylor gas bubbles are passing the section of the pipe the liquid film is flowing downward along the pipe wall for a certain period. In the next period, when the liquid slug flows past this section of the pipe the liquid with many small bubbles will flow upwards along the pipe wall. As the liquid is shed from the falling film it is essentially bubble free. This bubble free liquid once entering the liquid slug will squeeze some small gas bubbles towards the wall, where the



bubbles break. This will cause cavitation problems as part of the story. On the other hand, the periodic up and down film flow will probably cause fatigue of the corrosion product film. Modelling such a process will be very practical in the prediction of localized corrosion rates. By the same token, in annular flow some gas bubbles may also be trapped in the film, especially at pipe joints, where the strongest turbulent eddies appear and may trap many small gas bubbles in the liquid film and where localized corrosion occurred most frequently. This forms a sharp contrast to the belief that pitting corrosion only occurs when stagnant solutions exist. Other forms of localized corrosion are also worth exploring.

#### Modeling of the Gas Wells with Condensate

This work probably involves the distribution of the two liquid phases. Generally speaking, only when the water phase is contacting the metal wall will corrosion occur. However, the prediction of the probability of the water phase contacting the wall is not an easy job.

#### Prediction of the Effect of the Inhibitor

This point is very similar to point 2). Here, the main concern is to predict whether there is a thin

inhibitor film flowing along the wall. This work has theoretical significance far beyond the prediction of corrosion itself since the correct theory can also be applied to an area such as drag reduction. Practically, it is very important to the corrosion engineer to judge how much inhibitor should be used and length of time to use the inhibitor.

### Experimental Research on the Corrosion

#### Rate under Slug Flow

The significance of this research is not because little corrosion rate measurement work has been done in this flow regime and it is not because of its practical importance, but, because the information about the causes of high localized corrosion rates and the understanding of the mechanisms of corrosion in this flow regime is of enormous importance.

## REFERENCES

- Back, D. D. and McCready, M. J. "Theoretical Study of Interfacial Transport in Gas-Liquid Flows," *AIChE J.*, **34**, 1789-1802 (1988).
- Bacon, T. S. and Brown, E. A. "Corrosion in Distillate Wells," *Oil And Gas J.* **41**, No. 49, 91-92, (1943).
- Bard, A. J. and Faulkner, L. R. *Electrochemical Methods: Fundamental and Applications*, John Wiley, New York, 429-433, (1980).
- Bergles, A. E., Collier, J. G., Delhaye, J. M., Hewitt, G. F. and Mayinger, F. *Two-Phase Flow and Heat Transfer in the Power and Process Industries*, Hemisphere Publishing Corp., New York, 163-164 (1981).
- Bockris, J. O'M., Drazic, D. and Despic, A. R. "The Electrode Kinetics of the Deposition and Dissolution of Iron," *Electrochimica Acta*, **4**, 325-361 (1961).
- Bolmer, P. W. "Polarization of Iron in H<sub>2</sub>S-NaHS Buffers," *Corrosion*, **23**(3), 69-75 (1965).
- Bradburn, J. B. "Water Production — an Index to Corrosion" South Central NACE Meeting, Houston, Texas, (1977).
- Bradley, D. J. and Pitzer, K. S. "Thermodynamics of Electrolytes. 12. Dielectric Properties of Water and Debye-Huckel Parameters to 350 °C and 1 kbar," *J. Phys. Chem.*, **83**, 1599-1603 (1979).
- Burke, P. A. and Hausler, R. H. "Assessment of CO<sub>2</sub> Corrosion in the Cotton Valley Limestone Trend," *Advances in CO<sub>2</sub> Corrosion*, Vol. 2, (Burke, P. A., Symposium Chairman, and Asphahani, A. I. and Wright, B. S., Symposium Co-Chairmen, respectively) National Association of Corrosion Engineers, Houston, Texas, 133-160 (1985).
- Burke, P. A., Asphahani, A. I. and Wright, B. S. *Advances in CO<sub>2</sub> Corrosion*, Volume 2, NACE, Houston, Texas (1985).
- Butler, J. M. "Ionic Equilibrium - A Mathematical

- Approach," Addison-Wesley Publishing Company, Inc., Reading, Massachusetts, 206-320 (1964).
- Caussade, B., George, J. and Masbernat, L. "Experimental Study and Parameterization of Interfacial Gas Absorption," *AIChE. J.*, **36**, 265-274 (1990).
- Cebeci, T. and Smith, A. M. O. *Analysis of Turbulent Boundary Layers*, Academic Press, New York, 132-135 (1974).
- Chekhovich, V. Yu. and Pecherkin, N. I. "Heat and Mass Transfer and Wall Shear Stress in Vertical Gas-Liquid Flow," *Experl. Heat Transfer*, **1**, 253-264 (1987-1988).
- Chen, C. C., Britt, H. I., Boston, J. F. and Evans, L. B. "Local Composition Model for Excess Gibbs Energy of Electrolyte Systems," *AIChE J.* **28**, 588-596 (1982).
- Choi, H. J., Cepulis, R. L. and Lee, J. B. "Carbon Dioxide Corrosion of L-80 Grade Tubular in Flowing Oil-Brine Two-Phase Environments," *Corrosion*, **45**, 943-950 (1989).
- Conte, S. D. and De Boor, C. *Elementary Numerical Analysis: An Alogorithmic Approach*, Third Edition, McGraw-Hill Book Com., New York, 216-222 (1980).
- Crolet, J-L. "Acid Corrosion in Wells (CO<sub>2</sub>, H<sub>2</sub>S): Metallurgical Aspects," *J. Pet. Tech.*, **35**, 1553-1558 (1983).
- Crolet, J-L. and Bonis, M. R. "The Very Nature of the CO<sub>2</sub> Corrosion of Steels in Oil and Gas Wells and the Corresponding Mechanisms," *Oil Gas -European Magazine*, **2**, 68-76, (1984).
- Deberry, D. W. and Yost, A. "Corrosion Due to Use of Carbon Dioxide for Enhanced Oil Recovery," in *CO<sub>2</sub> Corrosion in Oil and Gas Production — Selected Papers, Abstract, and References*, (Newton Jr., L. E. Chairman, Hausler, R. H., Vice Chairman) NACE, Houston, Texas, 1-74 (1984).
- De Waard, C. and Milliams, D. E. "Carbonic Acid Corrosion of Steel," *Corrosion*, **31**, 177-181, (1975).
- Dobran, F. "Hydrodynamic and Heat Transfer Analysis of Two-Phase Annular Flow with a New Liquid Film Model of Turbulence," *Int. J. Heat Mass Transfer*, **26**, 1159-1171 (1983).

- Dunlop, A. K., Hassell, H. L. and Rhodes, P. R.  
"Fundamental Considerations in Sweet Gas Well Corrosion," in Advances in CO<sub>2</sub> Corrosion, Vol. 1, (R. H. Hausler, Symposium Chairman, H. P. Godard, Editor) National Association of Corrosion Engineers, Houston, Texas, 52-63 (1984).
- Edwards, T. J., Maurer, G., Newman, J. and Prausnitz, J. M.  
"Vapor-Liquid Equilibrium in Multicomponent Aqueous Solutions of Volatile Weak Electrolytes," AIChE J., 24, 966-976 (1978).
- Ellis, A. J. "Solubility of Calcite in Carbon Dioxide Solutions," Am. J. Sci., 257, 354-365 (1959).
- Erbar, J. H. "Documentation of the GPA\*SIM Program," Gas Processors Association, Tulsa, Oklahoma (August 1980).
- Eriksrud, E. and Søntvedt, T. "Effect of Flow on CO<sub>2</sub> Corrosion rates in Real and Synthetic Formation Waters," in Advances in CO<sub>2</sub> Corrosion, Vol. 1, (R. H. Hausler, Symposium Chairman, H. P. Godard, Editor) National Association of Corrosion Engineers, Houston, Texas, 20-38 (1984).
- Evans, U. R. The Corrosion and Oxidation of Metals: Scientific Principles and Practical Applications, St Martins Press Inc., New York, 868-882 (1960).
- Ewing, S. P. "Electrochemical Studies of the Hydrogen Sulfide Corrosion Mechanism," Corrosion, 11, 497t-501t (1955).
- Fang, C. S., Garbar, J. D., Perkins, R. and Reinhardt, J. R. "Computer Model of a Gas Condensate Well Containin Carbon Dioxide," Corrosion/89, Paper No. 465, New Orleans, Louisiana (1989).
- Galvele, J. R. "Pitting Corrosion," in Treatise on Materials Science and Technology, Vol. 23, Corrosion: Aqueous Processes and Passive Films (Edited by Scully, J. C.), Academic Press, New York, 1-57 (1983).
- Gatzke, L. K. and Hausler, R. H. "A Novel Correlation of Tubing Corrosion Rates in Deep, Hot Gas Well with Water and Gas Production Rates," in Advances in CO<sub>2</sub> Corrosion, Vol. 1, (R. H. Hausler, Symposium Chairman, H. P. Godard, Editor) National Association of Corrosion Engineers, Houston, Texas, 87-102, (1984).
- Greco, E. C. and Wright, W. B. "Corrosion of Iron in an H<sub>2</sub>S-CO<sub>2</sub>-H<sub>2</sub>O System," Corrosion, 18, 119t-124t (1962).

- Geelen, Ir. P. M. H. and Groenewoud, K. "Internal Corrosion of Oil and Gas Conduits and its Prevention in the Netherlands," The Sixth European Congress on Metallic Corrosion, 1977, in CO<sub>2</sub> Corrosion in Oil and Gas Production, 456-462 (Compiled and Edited by NACE Task Group T-1-3, Newton Jr., L. E. Chairman, Hausler, R. H., Vice Chairman) National Association of Corrosion Engineers, Houston, Texas (1984).
- Granville, P. S. "A Near-Wall Eddy Viscosity Formula for Turbulent Boundary Layers in Pressure Gradients Suitable for Momentum, Heat, or Mass Transfer," J. Fluids Eng., 112, 240-243 (1990).
- Gray, L. G. S., Anderson, B. G., Danysh, M. J. and Tremaine, P. R. "Mechanisms of Carbon Steel Corrosion in Brines Containing Dissolved Carbon dioxide at pH 4," Corrosion/89, Paper No. 464, New Orleans, Louisiana (1989).
- Greene N. D. and Fontana, M. G. "A Critical Analysis of Pitting Corrosion," Corrosion, 15, 25t-31t (1959).
- Hachermann, N. and Shock, D. A. "Surface Layers on Steel in Natural Gas Condensate Wells," Ind. Eng. Chem., 39(7), 863-867, (1947).
- Hassler, R. H. "The Mechanism of CO<sub>2</sub> Corrosion of Steel in Hot, Deep Gas Wells," in Advances in CO<sub>2</sub> Corrosion, Vol. 1, (R. H. Hausler, Symposium Chairman, H. P. Godard, Editor) National Association of Corrosion Engineers, Houston, Texas, 72-86 (1984).
- Hausler, R. H. and Burke, P. A. "Corrosion Monitoring in Sweet Production: Field Experiences with Iron Counts, Coupons and Calipers," in Advances in CO<sub>2</sub> Corrosion, Vol. 2, (Burke, P. A., Symposium Chairman, and Asphahani, A. I. and Wright, B. S., Symposium Co-Chairmen, respectively) National Association of Corrosion Engineers, Houston, Texas, 161-192 (1985).
- Hausler, R. H. and Godard, H. P. Advances in CO<sub>2</sub> Corrosion, Vol. 1, NACE, Houston, Texas (1984).
- Henstock, W. H. and Hanratty, T. J. "The Interfacial Drag and the Height of the Wall Layer in Annular Flows," AIChE. J., 22, 990-1000 (1976).
- Hinze, J. O. Turbulence, McGraw-Hill Book Com., Second Edition, New York, 622 (1975).

- Houghton, C. J. and Westermarck, R. V. "North Sea Downhole Corrosion: Identifying the Problem; Implementing the Solutions," *J. Pet. Tech.*, 35, 239-246 (1983).
- Hudson, T. E. "Understanding and Controlling Corrosivity of Heavyweight Brines," *SPE Production Engineering*, 4, 184-188 (1989).
- Ikeda, A., Ueda, M and Mukai, S. "CO<sub>2</sub> Behavior of Carbon and Cr Steels," in *Advances in CO<sub>2</sub> Corrosion*, Vol. 1, (R. H. Hausler, Symposium Chairman, H. P. Godard, Editor) National Association of Corrosion Engineers, Houston, Texas, 39-51, (1984).
- Ikeda A., Ueda, M. and Mukai, S. "Influence of Environment Factors on Corrosion in CO<sub>2</sub> Source Well," in *Advances in CO<sub>2</sub> Corrosion*, Vol. 2, (Burke, P. A., Symposium Chairman, and Asphahani, A. I. and Wright, B. S. Symposium Co-Chairmen, respectively) National Association of Corrosion Engineers, Houston, Texas, 1-22 (1985).
- Iyer, R. N., Takeuchi, I., Zamanzadeh, M. and Pichering, H. W. "Hydrogen Sulfide Effect on Hydrogen Entry into Iron — A Mechanistic Study," *Corrosion*, 46, 460-468 (1990).
- Jacobson, R. L. and Langmuir, D. "Dissociation Constants of Calcite and CaHCO<sub>3</sub><sup>+</sup> from 0 to 50°C," *Geochimica et Cosmochimica Acta*, 38, 301-318 (1974).
- Jagota, A. K., Rhodes, E. and Scott, D. S. "Mass Transfer in Upwards Co-current Gas-Liquid Annular Flow," *Chem. Eng. J.*, 5, 23-31 (1973).
- Jasinski, R. "Corrosion of N80-Type Steel by CO<sub>2</sub>/Water Mixtures," *Corrosion*, 43, 214-218 (1987).
- Johnson B. V., Choi, H. J. and Green, A. S. "Effects of Liquid Wall Shear Stress on CO<sub>2</sub> Corrosion of X-52 C-Steel in Simulated Oilfield Production Environments," *Corrosion/91*, Paper No. 573, Cincinnati, Ohio (1991).
- Kasturi, G. and Stepanek, J. B. "Two-Phase Flow-IV. Gas and Liquid Side Mass Transfer Coefficients," *Chem. Eng. Sci.*, 29, 1849-1856 (1974).
- Kawashima, A., Hashimoto, K. and Shimodaira, S. "Hydrogen Electrode Reaction and Hydrogen Embrittlement of Mild Steel in Hydrogen Sulfide Solutions," *Corrosion*, 32, 321-331 (1976).

- Kawazuishi, K. and Prausnitz, J. M. "Correlation of Vapor-Liquid Equilibria for the System Ammonia-Carbon Dioxide-Water," *Ind. Eng. Chem. Res.*, **26**, 1482-1485 (1987).
- Kerr, C. P. "Chemical Equilibria in Flue Gas Scrubbing Slurries," in *Thermodynamics of Aqueous Systems with Industrial Applications* (Newman, S. A. Editor), ACS Symposium Series 133, ACS, Washington, D. C., 91-106 (1980).
- Langmuir, D. "Stability of Calcite Based on Aqueous Solubility Measurements," *Geochimica et Cosmochimica Acta*, **32**, 835-851 (1968).
- Levich, V. G. *Physicochemical Hydrodynamics*, Prentice-Hall Inc., Englewood Cliffs, N. J., 166 (1962).
- Lin, C. S., Moulton, R. W. and Putnam, G. L. "Mass Transfer between Solid Wall and Fluid Streams: Mechanism and Eddy Distribution Relationship in Turbulent Flow," *Ind. Eng. Chem.*, **45**, 636-640 (1953).
- Liu, G. and Erbar, R. C. "Detailed Simulation of Gas Well Downhole Corrosion in Carbon Steel Tubulars," *Corrosion/90*, Paper No. 30, Las Vegas, Nevada (1990).
- Mahato, B. K. and Shemilt, L. W. "Effect of Surface Roughness on Mass Transfer," *Chem. Eng. Sci.*, **23**, 183-185, (1968).
- Martin, R. L. "Corrosion of Alloy Steels in Oil Field Fluids," *Corrosion*, **44**, 916-920 (1988).
- Masmura, K., Hashizume, S., Nunomura, K., Sakai, J. and Matsushima, I. "Corrosion of Carbon and Alloy Steels in Aqueous CO<sub>2</sub> Environments," in *Advances in CO<sub>2</sub> Corrosion*, Vol. 1, (R. H. Hausler, Symposium Chairman, H. P. Godard, Editor) National Association of Corrosion Engineers, Houston, Texas, 143-150 (1984).
- McCready, M. J. and Hanratty, T. J. "Effect of Air Shear on Gas Absorption by a Liquid Film," *AIChE J.*, **31**, 2066-2074 (1985).
- McCready, M. J., Vassiliadou, E. and Hanratty, T. J. "Computer Simulation of Turbulent Mass Transfer at a Mobile Interface," *AIChE J.*, **32**, 1108-1115 (1986).
- Meyer, F. H., Riggs, O. L., Mcglasson, R. L. and Sudbury, J. D. "Corrosion Products of Mild Steel in Hydrogen



- Sulfide Environments," Corrosion, 14, 109t-115t (1958).
- Mizushina, T., Ogino, F., Oka, Y. and Fukuda, H. "Turbulent Heat and Mass Transfer between Wall and Fluid Streams of Large Prandtl and Schmidt Numbers," Int. J. Heat Mass Transfer, 14, 1705-1716 (1971).
- Morris, D. R., Sampaleanu, L. P. and Veysey, D. N. "The Corrosion of Steel by Aqueous Solutions of Hydrogen Sulfide," J. Electrochem. Soc., 127, 1228-1235 (1980).
- Na, T. Y., Computational Methods in Engineering Boundary Value Problems," Academic Press, New York, 84-85 (1979).
- Newton, L. E. and Hausler, R. H. CO<sub>2</sub> Corrosion in Oil and Gas Production- Selected Paper, Abstracts, and References, NACE, Houston, Texas (1984).
- Ogundele, G. I. and White, W. E. "Some Observations on Corrosion of Carbon Steel in Aqueous Environments Containing Carbon Dioxide," Corrosion, 42, 71-78 (1986).
- Ogundele, G. I. and White, W. E. "Observations on the Influences of Dissolved Hydrocarbon Gases and Variable Water Chemistries on Corrosion of API-L80 Steel," Corrosion, 43, 665-673 (1987).
- Palacios C. A. and Shadley, J. R. "Characteristics of Corrosion Scales on Steels in a CO<sub>2</sub>-Saturated NaCl Brine," Corrosion, 47, 122-127 (1991).
- Plummer, L. N. and Busenberg, E. "The Solubilities of Calcite, Aragonite and Vaterite in CO<sub>2</sub>-H<sub>2</sub>O Solutions between 0 and 90 °C and an Evaluation of the Aqueous Model for the System CaCO<sub>3</sub>-CO<sub>2</sub>-H<sub>2</sub>O," Geochimica et Cosmochimica Acta, 46, 1011-1040 (1982).
- Postlethwaite, J. and Lotz, U. "Mass transfer at Erosion-Corrosion Roughened Surfaces," Can. J. Chem. Eng., 66, 75-78 (1988).
- Pound, B. G., Wright, G. A. and Sharp, R. M. "The Anodic Behavior of Iron in Hydrogen Sulfide Solutions," Corrosion, 45, 386-392 (1989).
- Pouson, B. "Electrochemical Measurements in Flowing Solutions," Corrosion Science, 23, 391-430 (1983).
- Reinhardt, J. R. and Powell, T. S. "Corrosion Reduction in

- Production Tubing with the Aid of a Phase Equilibrium Model," SPE Production Engineering, 3, 591-596 (1988).
- Rhodes, F. H. and Clark Jr., J. M. "Corrosion of Metals: by Water and Carbon Dioxide under Pressure," Ind. Eng. Chem., 28, 1078-1079 (1936).
- Rice P. W. "Selecting Metallic Materials for Downhole Service," World Oil, 208, No. 6, 70-76 (Nov. 1989).
- Robertson, C. C., "DOWN\*HOLE Phase I: A Computer Model for Predicting the Water Phase Corrosion Zone in Gas and Condensate Wells," Master Thesis, Oklahoma State University, Stillwater, Oklahoma (May 1988).
- Robertson, C. A. and Erbar, R. C. "Computer Simulation for Prediction of Downhole Corrosion," Corrosion/88, St Louis, (March 1988).
- Rogers, L. A., Varughese, K., Prestwlch, S. M., Waggett, G. G., Sallml, M. H., Oddo, J. E., Street Jr., E. H. and Tomson, M. B. "Use of Inhibitors for Scale Control in Brine-Producing Gas and Oil Wells," SPE Production Engineering, 5, 77-82 (1990).
- Ross, T. K. and Badhwar, P. K. "The Effect of Surface Roughness upon Electrochemical Processes," Corrosion Science, 5, 29-38 (1965).
- Sardisco, J. B. and Pitts, R. E. "Corrosion of Iron in an H<sub>2</sub>S-CO<sub>2</sub>-H<sub>2</sub>O System: Mechanism of Sulfide Film Formation and Kinetics of Corrosion Reaction," Corrosion, 21, 245-253 (1965).
- Sardisco, J. B., Wright, W. B. and Greco, E. C. "Corrosion of Iron in an H<sub>2</sub>S-CO<sub>2</sub>-H<sub>2</sub>O System: Corrosion Film Properties on Pure Iron," Corrosion, 19, 354t-359t (1963).
- Sato, N. "Toward a More Fundamental Understanding of Corrosion Processes," Corrosion, 45, 354-368 (1989).
- Schmitt, G. and Rothmann, B. "Studies on the Corrosion Mechanism of Unalloyed Steel in Oxygen-Free Carbon Dioxide Solutions: Part I. Kinetics of the Liberation of Hydrogen," Werkstoffe und Korrosion, 28, 816-824 (1977), in CO<sub>2</sub> Corrosion in Oil and Gas Production, 154-162, (Compiled and Edited by NACE Task Group T-1-3, Newton Jr., L. E. Chairman, Hausler, R. H., Vice Chairman) National Association of Corrosion Engineers, Houston, Texas (1984).

- Segnit, E. R., Holland, H. D. and Biscardi, C. J. "The Solubility of Calcite in Aqueous Solutions-I. The Solubility of Calcite in Water between 75° and 200° at CO<sub>2</sub> Pressures up to 60 Atm," *Geochimica et Cosmochimica Acta*, **26**, 1301-1331 (1962).
- Sheosmith, D. W., Taylor, P., Bailey, M. G., and Owen, D. G. "The Formation of Ferrous Monosulfide Polymorphs during the Corrosion of Iron by Aqueous Hydrogen Sulfide at 21°C," *J. Electrochem. Soc.*, **127**, No. 5, 1007-1015, (1980).
- Shock, D. A. and Sudbury, J. D. "Prediction of Corrosion in Oil and Gas Wells," *World Oil*, **133**, 180-192 (1951).
- Smith, F. G. "Controlling Corrosion in Deep South Louisiana Gas Wells," *World Oil*, **195**(6), 77-79, (Nov. 1982).
- Speel, L. "Corrosion Control in German Gas Wells," *Materials Performance*, **15**, No. 8, 46-53 (1976).
- Tewari, P. H. and Campbell, A. B. "Dissolution of Iron During the Initial Corrosion of Carbon Steel in Aqueous H<sub>2</sub>S solutions," *Can. J. Chem.*, **57**, 188-196 (1979).
- Thompson, R. M., Kohut, G. B., Canfield, D. R. and Bass, W. R. "Sulfide Stress Cracking Failures of 12Cr and 17-4PH Stainless Steel Wellhead Equipment," *Corrosion*, **47**, 216-220 (1991).
- Tuttle, R. N. "Corrosion in Oil and Gas Production," *J. Pet. Tech.*, **39**, 756-762 (1987).
- Tuttle, R. N. "What Is a Sour Environment?" *J. Pet. Tech.*, **42**, 260-262 (1990).
- Tuttle, R. N. and Kane, R. D., *H<sub>2</sub>S Corrosion in Oil & Gas Production - A Compilation of Classic Papers*, NACE, Houston, Texas (1981).
- Valand, T. and Sjøwall, P. A. "Properties and Composition of Surface Films Formed on Steel in CO<sub>2</sub>-Aqueous Solutions," *Electrochimica Acta*, **34**, 273-279 (1989).
- Vetter, G. *Electrochemical Kinetics*, Academic Press, New York, 759 (1967).
- Videm, K. and Dugstad, A. "Effect of Flow Rate, pH, Fe<sup>++</sup> Concentration and Steel Quality on the CO<sub>2</sub> Corrosion of Carbon Steels," *Corrosion/87*, Paper No. 42, San Francisco, California (1987).

- Vulchanov, N. L. and Zimparov, V. D. "Stabilized Turbulent Fluid Friction and Heat Transfer in Circular Tubes with Internal Sand Type Roughness at Moderate Prandtl Numbers," *Int. J. Heat Mass Transfer*, **32**, 29-34 (1989).
- Wasdon, F. K. and Dukler, A. E. "A Numerical Study of Mass Transfer in Free Falling Wavy Films," *AIChE J.* **36**, 1379-1390 (1990)
- Weeter, R. F. "A Case History — High Pressure Sour Gas Well Corrosion Control — Brown Bassett Field," *Proceedings of the 11th Annual Southwestern Short Course, NACE*, 55-60 (April 1964).
- Wieckowski, A., Ghali, E., Szklarczyk, M., and Sobkowski, J. "The Behaviour of Iron Electrode in CO<sub>2</sub> -Saturated Neutral Electrolyte — I. Electrochemical Study," *Electrochimica Acta*, **28**, 1619-1626 (1983a).
- Wieckowski, A., Ghali, E., Szklarczyk, M., and Sobkowski, J. "The Behaviour of Iron Electrode in CO<sub>2</sub> -Saturated Neutral Electrolyte — II. Radiotracer Study and Corrosion Considerations," *Electrochimica Acta*, **28**, 1627-1633 (1983b).
- Wikjord, A. G., Rummary, T. E., Doern, F. E. and Owen, D. G. "Corrosion and Deposition during the Exposure of Carbon Steel to Hydrogen Sulfide-Water Solutions," *Corrosion Science*, **20**, 651-671 (1980).
- Xia, Z., Chou, K-C. and Szklarska-Smialowska, Z. "Pitting Corrosion of Carbon Steel on CO<sub>2</sub>-Containing NaCl Brine," *Corrosion*, **45**, 636-642 (1989).
- Zemaitis, Jr. J. F., Clark, D. M., Rafal, M. and Scrivner, N. C., *Handbook of Aqueous Electrolyte Thermodynamics: Theory & Application*, "DIPPR, New York, 586-587 (1986).
- Zitter, H. "Corrosion Phenomena in Sour Gas Wells," *Erdoel-Erdgas-Zeitschrift*, **89**(3), 101-106 (1973).

2

VITA

GUOHAI LIU

Candidate for the Degree of  
Doctor of Philosophy

Thesis: A MATHEMATICAL MODEL FOR PREDICTION OF DOWNHOLE  
GAS WELL UNIFORM CORROSION IN CO<sub>2</sub> AND H<sub>2</sub>S  
CONTAINING BRINES

Major Field: Chemical Engineering

Biographical:

Personal Data: Born in Hebei Province, People's  
Republic of China, November 2, 1955, the son of  
Shuqing and Guangsheng Liu.

Education: Graduated from Yutian High School, Hebei  
Province, PRC., in January 1973; received  
Bachelor of Science Degree in Chemical  
Engineering from East China Institute of Chemical  
Technology, Shanghai, China, in January 1982;  
received Master of Science Degree in Chemical  
Engineering from Central Coal Mining Research  
Institute, Beijing, China, in December 1984;  
completed requirements for the Doctor of  
Philosophy Degree at Oklahoma State University in  
December 1991.

Professional Experience: Research Assistant, School  
of Chemical Engineering, Oklahoma State  
University, August 1988 to August 1991; Research  
Engineer and Group Head, Beijing Research  
Institute of Coal Chemistry at Central Coal  
Mining Research Institute, Beijing, China, from  
December 1984 to August 1988.